Trajectory Tracking and Formation Control of a Platoon of Mobile Robots

Mahsa Aliakbar Golkar

A Thesis

in

The Department

of

Electrical and Computer Engineering

Presented in Partial Fulfillment of the Requirements

for the Degree of Master of Applied Science at

Concordia University

Montréal, Québec, Canada

July 2010

Your file Votre référence
ISBN: 978-0-494-71021-0
Our file Notre référence
ISBN: 978-0-494-71021-0

ABSTRACT

Trajectory Tracking and Formation Control of a Platoon of Mobile Robots

Mahsa Aliakbar Golkar

This thesis is concerned with controlling a platoon of wheeled mobile robots (WMR), where the robots are aimed to follow a trajectory while they maintain their formation intact. The control design is carried out by considering unicycle kinematics for each robot, and the leader-follower structure for the formation. It is assumed that every robot except the one located at the end of each platoon can potentially be the leader to the one behind it. It is also assumed that each follower is capable of sensing its relative distance and relative velocity with respect to its preceding robot. The stability of the proposed control law is investigated in the case of perfect sensing and in the presence of input saturation. The impact of measurement noise on the followers is then studied assuming that a known upper bound exists on the measurement error, and a linear matrix inequality (LMI) methodology is proposed to design a control law which minimizes the upper bound on the steady-state error.

The problem is then investigated in a more practical setting, where the control input is subject to delay, and that the tracking trajectory can be different in distinct time intervals. It is to be noted that delay often exists in this type of cooperative control system due to data transmission and signal processing, and if neglected in the control design, can lead to poor closed-loop performance or even instability. Furthermore, switching in tracking trajectory can be used as a collision avoidance strategy in the formation control problem. Delay dependent stability conditions are derived in the form of LMIs, and the free-weighting matrix approach is used to obtain less conservative results. Simulations are presented to demonstrate the efficacy of the results obtained in this thesis.

To my parents

for their love and support

ACKNOWLEDGEMENTS

This work would not be possible without help and encouragement I received from several people. First and foremost, I would like to express my most sincere gratitude to my supervisor, Dr. Amir G. Aghdam for his continuous patience, support and guidance in the development of this thesis. I have benefited greatly from his experiences.

My appreciation also goes to my co-supervisor, Dr. Iraj Mantegh from NRC (National Research Council of Canada) for supporting this research and providing me with valuable discussions.

My gratitude extends to my colleagues at Concordia University and my friends in Montreal whose friendship means a lot to me. In particular, I would like to thank Dr. Ahmadreza Momeni, postdoctoral fellow in Concordia University, for providing me with invaluable discussion and sharing the wealth of knowledge and experience. I would also like to appreciate my friend Dr. Kaveh Moezzi, postdoctoral fellow in Concordia University, for detailed discussion in area of delayed and switched systems.

Last, but not least, I should thank my dear parents who have always been present throughout my life in spite of the distance and also my lovely sister and brother, Noushin and Alireza for their support.

TABLE OF CONTENTS

List of Figures

List of Abbreviations

WMR	Wheeled Mobile Robot
LMI	Linear Matrix Inequality
LTI	Linear Time-Invariant
TDS	Time-Delay System

Chapter 1

Introduction

1.1 Motivation

Robotics as an engineering field has proved its efficiency in the industrial manufacturing world. The advantages of using robots instead of humans for performing some specific tasks (e.g., handling hazardous material) have attracted many researchers. This research is mainly focused on the mobile robots.

Mobile robots can move in a number of ways. Walking, jumping, sliding and rolling are a few examples. Generally, mobile robots locomate using either wheeled mechanism or a number of legs. Legged mobile robots are capable of crossing a hole or chasm and manipulating objects. However, compared to the wheeled mobile robots (WMR), this type of robot is of greater mechanical complexity, due to its higher degree of freedom. Figures 1.1, 1.2, 1.3 and 1.4 show some examples of legged robots with different number of legs [1].

In contrast to legged mobile robots, on the other hand, WMRs have their own advantages too. First of all, they have a simpler structure. Furthermore, they are well-suited for flat grounds, and are more stable statically. The latter property is due to the fact that the minimum number of wheels required for a mobile robot to be statically stable is

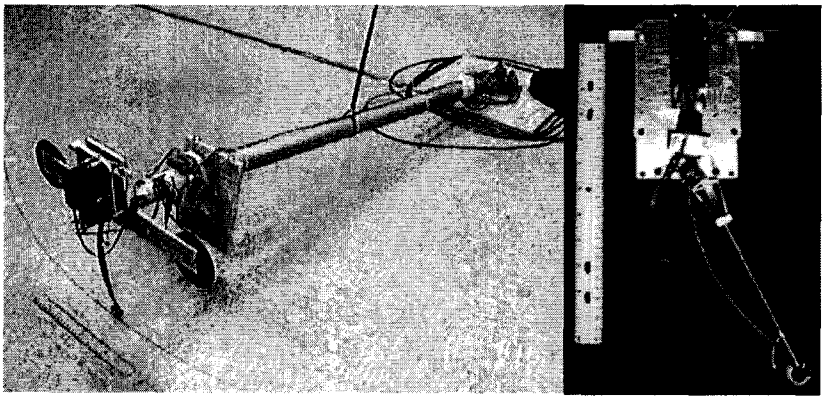

Figure 1.1: The 2D single bow leg hopper [1].

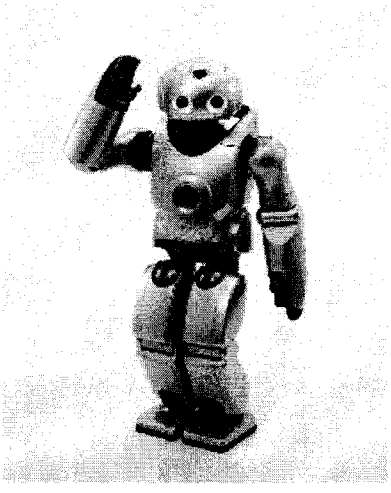

Specifications:

Weight:	7 kg
Height:	58 cm
Neck DOF:	4
Body DOF:	2
Arm DOF:	2 x 5
Legs DOF:	2 x 6
Five-finger Hands	

Figure 1.2: The Sony SDR-4X II, Sony Corporation [1].

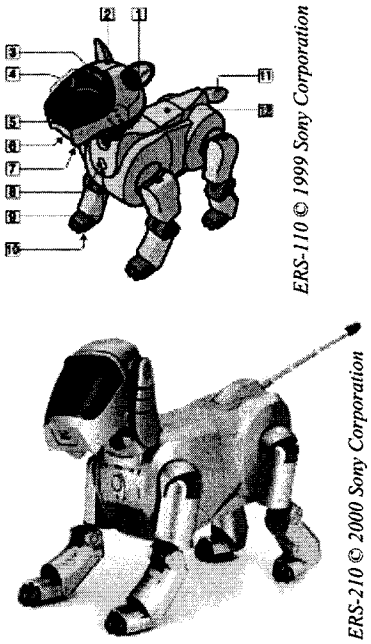

1 Stereo microphone: Allows AIBO to pick up surrounding sounds.
2 Head sensor: Senses when a person taps or pets AIBO on the head.
3 Mode indicator: Shows AIBO's operation mode.
4 Eye lights: These light up in blue-green or red to indicate AIBO's emotional state.
5 Color camera: Allows AIBO to search for objects and recognize them by color and movement.
6 Speaker: Emits various musical tones and sound effects.
7 Chin sensor: Senses when a person touches AIBO on the chin.
8 Pause button: Press to activate AIBO or to pause AIBO.
9 Chest light: Gives information about the status of the robot.
10 Paw sensors: Located on the bottom of each paw.
11 Tail light: Lights up blue or orange to show AIBO's emotional state.
12 Back sensor: Senses when a person touches AIBO on the back.

Figure 1.3: AIBO, the artificial dog from Sony, Japan [1].

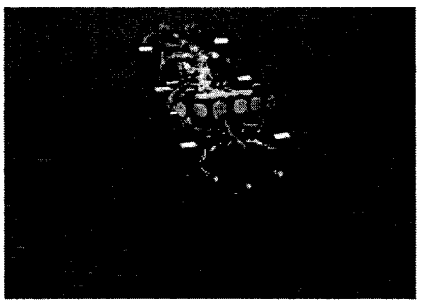

Figure 1.4: Genghis, one of the most famous walking robots from MIT, uses hobby servomotors as its actuators (http://www.ai.mit.edu/projects/genghis). MIT AI Lab [1].

two [1]. There exist different types of WMRs. For single-body robots, for example, the most commonly used ones are known to be differential drive and synchro drive, tricycle or car-like drive, and omnidirectional steering. Figures 1.5, 1.6, 1.7, 1.8 and 1.9 show a few examples of wheeled mobile robots.

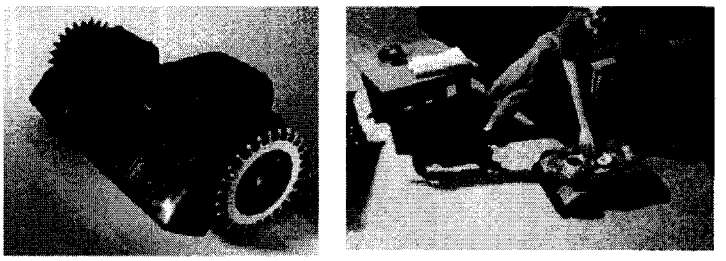

Figure 1.5: Cye, a commercially available domestic robot that can vacuum and make deliveries in the home, is built by Aethon Inc. (http://www.aethon.com) [1].

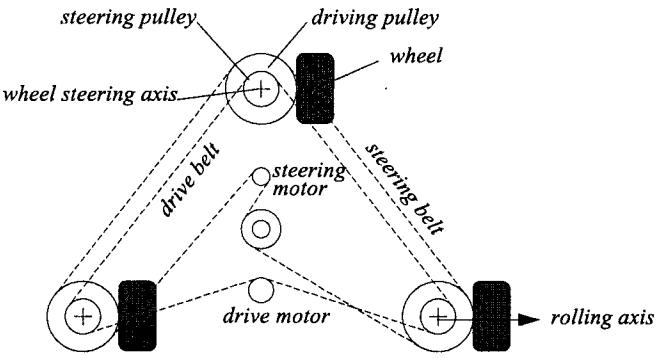

Figure 1.6: Synchro drive. It has the ability to move in any direction [1].

There has been a large increase in the use of WMRs in industry in recent years. This is more evident for the cases where autonomous motion capabilities are required over reasonably smooth grounds and surfaces. The problem of motion planning and control of WMRs, which pose several theoretical and practical challenges, have been extensively studied in the literature; e.g., see [2–4]. A detailed study on kinematics of WMRs can be found in [5].

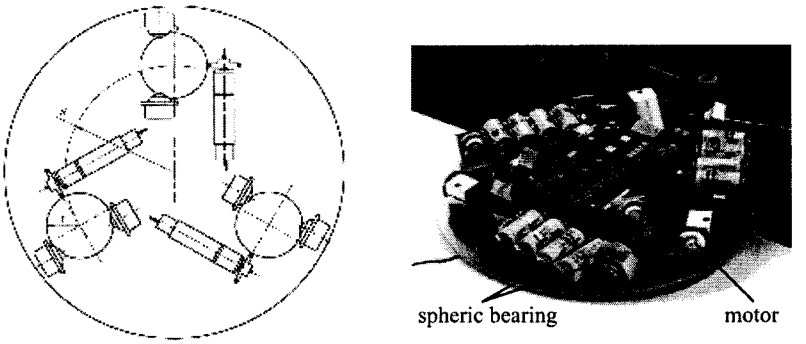

Figure 1.7: The Tribolo designed at EPFL (Swiss Federal Institute of Technology, Lausanne, Switzerland. Left: arrangement of spheric bearings and motors (bottom view). Right: Picture of the robot without the spherical wheels (bottom view) [1].

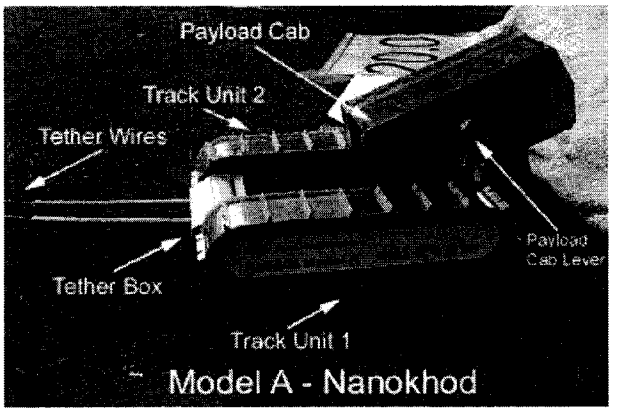

Figure 1.8: The microrover Nanokhod, developed by von Hoerner and Sulger GmbH and the Max Planck Institute, Mainz, for the European Space Agency (ESA) [1].

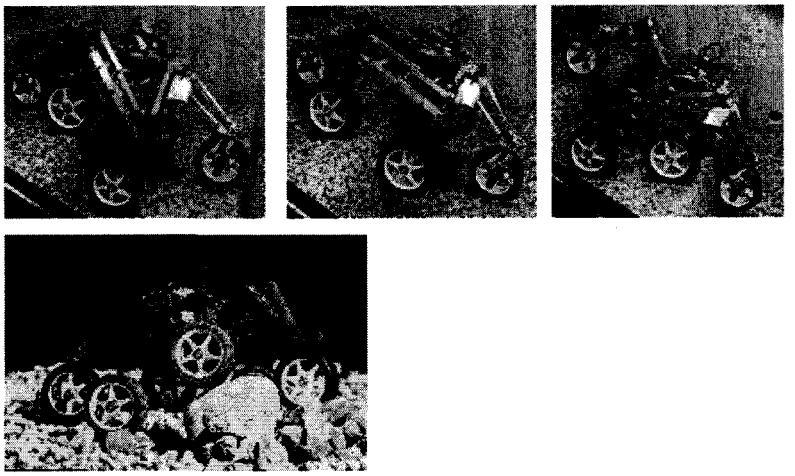

Figure 1.9: Shrimp, an all-terrain robot with outstanding passive climbing abilities [1].

To control a robot, it is required to have specific information about its actuator and also some knowledge of its environment and relevant signals. The latter requirement emphasizes the importance of studying different types of sensors and choosing the proper one based on the specific application and desired performance. Siegwart and Nourbakhsh in [1] studied different types of sensors used in mobile robots, and discussed their advantages and disadvantages. A brief description of the different sensors used in mobile robots is summarized below.

1.2 Sensors for Mobile Robots

There is a wide range of sensors available for robots in industry. Some sensors are used for simple measurements such as internal temperature of a robot's electronics or rotational speed of the motor, while others are used for more complex measurements such as those involving environment, e.g., robot's global position. A mobile robot is usually accompanied with a wide variety of sensors, as depicted in Figure 1.10.

Nourbakhsh and Siegwart in [1] classified robot sensors as proprioceptive or exteroceptive and passive or active, as described below.

- Proprioceptive/Exteroceptive

    i) Proprioceptive sensors are those which measure values internal to the system (robot), such as motor speed and wheel load.

    ii) Exteroceptive sensors are those which measure the information related to the environment, such as distance and light intensity.

- Passive/Active

    i) Passive sensors measure natural ambient energy entering the sensor [6]. Examples of this type of sensor include temperature probes and microphones.

    ii) Active sensors measure a quantity such as distance by emitting a signal and detecting its reflection [6]. Examples of active sensors include laser range-finders, and ultrasonic sensors used for medical diagnostic.

Sensors have different levels of performance. Typically, the more expensive the sensor is, the more accurate its measurements are. Hence, the choice of sensor is normally made based on the specific application and desired performance. Usually the sensor performance is described by a variety of characteristics, including dynamic range, resolution, linearity, sensitivity, cross-sensitivity, accuracy and precision. The most useful sensors for mobile robots are briefly discussed below [1].

- Wheel/motor Sensors: Wheel/motor sensors are used for measuring the values related to the internal state and dynamics of the robot. Although they generally have high-quality and excellent resolution, they are relatively low-cost. This is because of the wide use of such sensors in a broad range of other applications. One example of this type of sensor is the optical encoder.

- Heading Navigation Sensors: Heading sensors are used for determining the robot's orientation and inclination. Inertial navigation systems (INS), Gyroscopes, inclinometer and compass are a few examples of such sensors.

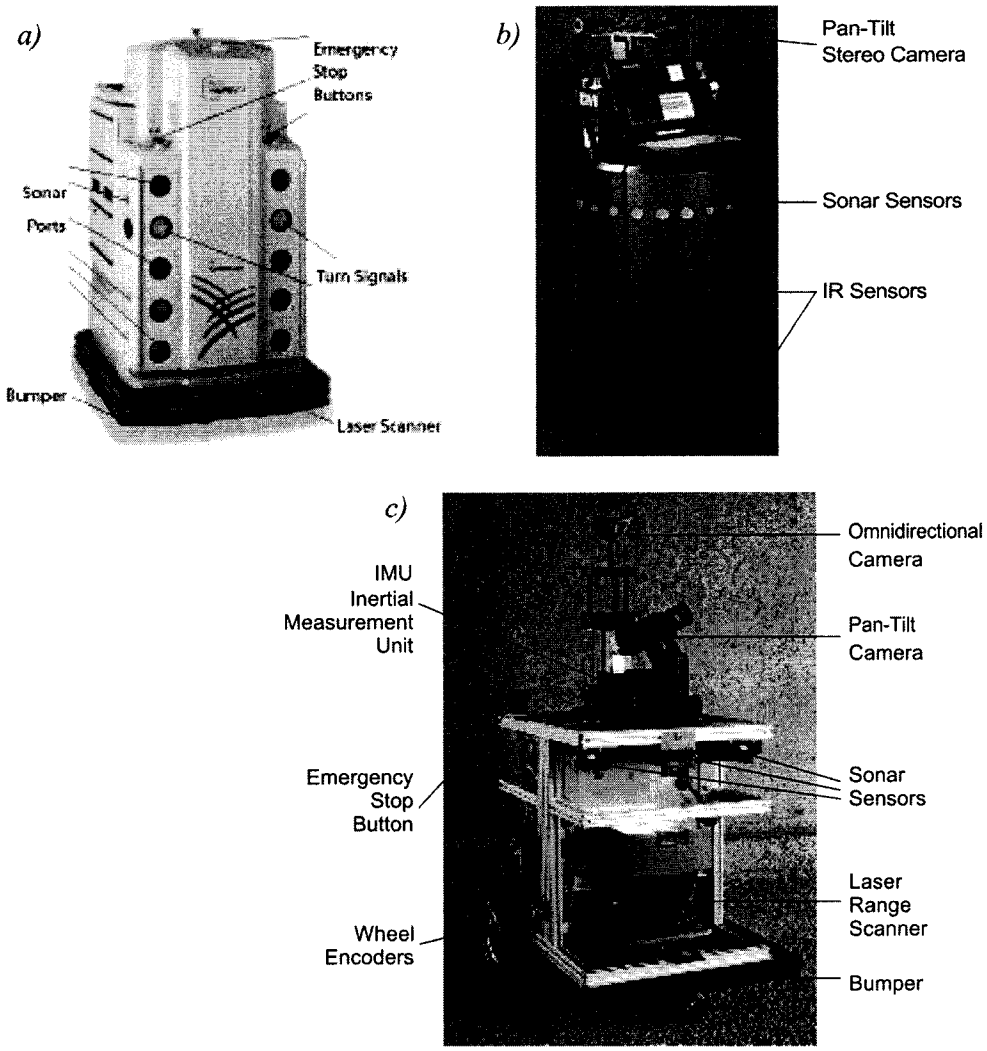

Figure 1.10: Examples of robots with multi-sensor systems: (a) HelpMate from Transition Research Cooperation; (b) B21 from Real World Interface; (c) BIBA robot, BlueBotices SA [1].

Figure 1.11: A digital compass as a heading sensor [1].

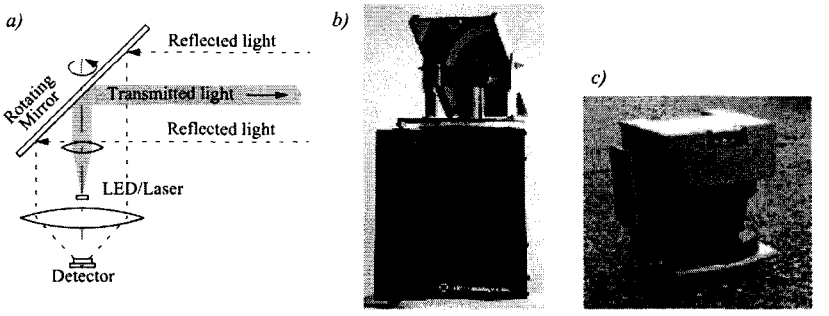

Figure 1.12: (a) Schematic drawing of a laser range sensor with rotating mirror; (b) a scanning range sensor from EPS Technologies Inc., and (c) an industrial 180-degree laser range sensor from Sick Inc., Germany [1].

- Ground-Based Beacons: These sensors are used for identifying the robot's location. A well-known example of such beacon systems is the global positioning system (GPS).

- Active Range-Sensors: This is another type of sensor used for determining the robot's location. The main advantage of these sensors is their low cost. Active range-sensors are the most common type of sensors used in mobile robots. Ultrasonic sensors, laser-range finder, laser detection and ranging (LADAR), and the optical triangulation sensor are some examples of active range-sensors.

- Motion/Speed Sensors: These sensors measure the relative motion between the robot and its environment. They are used in applications where obstacle avoidance is of interest. The pyroelectric sensor is an example of this type of sensor.

- Vision-Based Sensors: These sensors provide a wide variety of information about

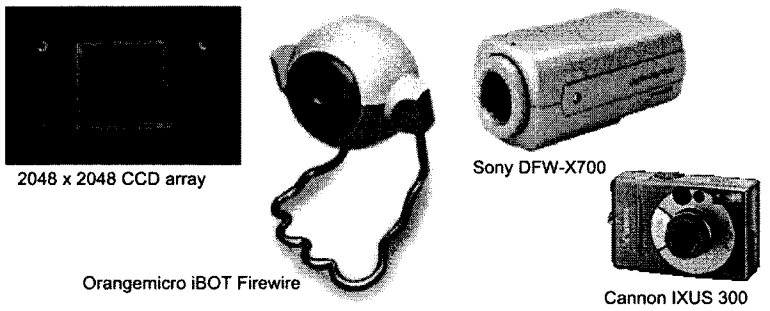

Figure 1.13: Commercially available charged coupled device (CCD) chips and cameras [1].

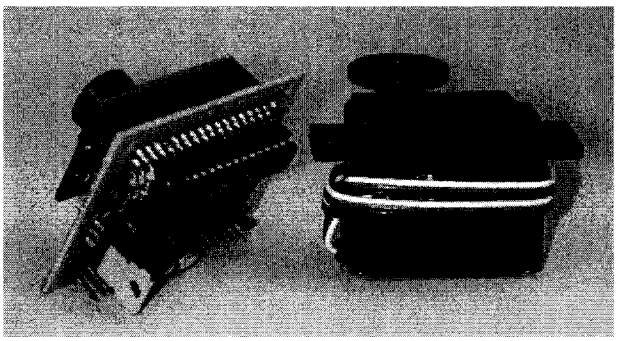

Figure 1.14: Vision-Based Sensor: The CMUcam sensor consists of three chips: a CMOS imaging chip, a SX28 microprocessor, and a Maxim RS232 level shifter [1].

the robot's environment. Therefore, these are also commonly used in applications where obstacle avoidance is required.

In Table 1.1, the important characteristics of different types of sensors are summarized. It is to be noted that sensor classes in Table 1.1 are arranged in an ascending order of complexity and descending order of technological maturity.

1.3 Controllability and Stabilizability of Mobile Robots

Some mobile robots are known to be nonholonomic due to their perfect rolling constraint [7]. Let (x, y, θ) represent the generalized coordinates of the system; then this constraint can be written as:

$$\dot{x}sin\theta - \dot{y}cos\theta = 0 \tag{1.1}$$

Representing the state-space as $q = [x, y, \theta]^T$, the first-order kinematics of a WMR is given by:

$$\begin{bmatrix} \dot{x} \\ \dot{y} \\ \dot{\theta} \end{bmatrix} = g_1(q)v + g_2(q)\omega = \begin{bmatrix} cos\theta \\ sin\theta \\ 0 \end{bmatrix} v + \begin{bmatrix} 0 \\ 0 \\ 1 \end{bmatrix} \omega \tag{1.2}$$

which can be expressed in the following general form:

$$\dot{q} = g_1 u_1 + g_2 u_2 \tag{1.3}$$

It is clear from (1.2) that g_1 and g_2 are two linearly independent vector fields. From Chow's theorem it is known that this system is controllable and can reach any arbitrary configuration in R^3.

Stability is the most important issue in the control of a WMR. The problem of stabilization of WMRs as nonholonomic systems is concerned with obtaining feedback laws which guarantee that an equilibrium of the closed-loop system is asymptotically stable. From the Brockett's necessary condition for feedback stabilization [8], it is known that there exists no smooth or continuous time-invariant static state feedback for this type of system to locally asymptotically stabilize any equilibrium point. In general, a nonholonomic system cannot be stabilized to an equilibrium using feedback linearization or any other control design approach that employs smooth time-invariant feedback. Nonsmooth or discontinuous time-invariant stabilization, time-varying stabilization and hybrid stabilization are the methods introduced in the literature to overcome this shortcoming of smooth time-invariant controllers. An extensive research on posture stabilization of nonholonomic systems using these methods can be found in [9–24].

1.4 Trajectory Tracking by Mobile Robots

Considering the nonholonomic dynamics of the system and difficulties in finding control input for posture stabilization of the system, it is often desirable to design control laws under which the system variables converge to a trajectory, rather than to a point. In this type of problem, the desired trajectory is predefined and the robot is to be controlled so that it asymptotically converges to the desired path. Various trajectory tracking methods are given in the literature. This includes using nonlinear feedback laws, dynamic feedback linearization, and backstepping approach, to name only a few. Extensive publication on trajectory tracking of nonholonomic systems such as mobile robots can be found in the literature (see e.g., [25–34]).

1.5 Formation Control of Mobile Robots

The earlier studies in the field of cooperative robots dates back to the 1980's. Since then, extensive research has been undertaken in this area, and a wide variety of related topics has been addressed. Coordination of multiple mobile robots, on the other hand, has attracted much interest recently. Exploiting a group of robots instead of a single robot or human for performing a prescribed spatially distributed task has significant advantages in various applications [3]. Some advantages and remarkable properties of multi-robot systems are [35]:

- higher efficiency;
- better performance;
- fault tolerance;
- wide range of application;
- robustness, and

- reduced cost.

Formation control is one of the most challenging research problems in cooperative mobile robots. This problem is concerned with a group of robots moving in formation and performing a single mission in a cooperative fashion. It is desired in this type of problem to control the relative position and orientation of the robots with respect to each other. Applications of formation control of cooperative robots include simultaneous localization and mapping, RoboCup (which is designed to play soccer and perform search and rescue), exploration of an unknown environment, and transportation of large objects, to name only a few [36–45]. The most effective techniques proposed in the literature for formation control of mobile robots are behavior-based, virtual-structure, and leader-follower.

1.5.1 Behavior-Based Approach

In the behavior-based approach, different possible behaviors are assigned to each robot [46], [47]. Based on the relative importance of each behavior, a weighting function is assigned to it [4]. This approach may be suitable for designing control strategies for robots with multiple competing objectives. Moreover, due to the decentralized structure of the control, it is a proper choice for systems with a large group of robots [3]. As a result, compared to other methods, a behavior-based approach may be implemented with significantly reduced communication requirement [48]. More precisely, the virtual-structure and leader-follower approaches (which will be described in the following subsections), require that the full state of the leader or virtual-structure be communicated to each member of the formation. A disadvantage of this approach, on the other hand, is the complexity of the mathematical stability analysis [3].

1.5.2 Virtual-Structure Approach

In the virtual-structure approach, the robot formation is considered as a single virtual rigid structure [49]. Desired trajectories are assigned to the entire formation as a whole instead of being assigned to each robot separately. Unlike the behavior-based approach, in this technique the behavior of the whole group is totally predictable and the formation may be maintained precisely; however, it requires heavier inter-robot communication [4]. An advantage of this method is known to be the possibility of attaining a certain degree of robustness of the formation to perturbations on the robots.

1.5.3 Leader-Follower Approach

In the leader-follower approach, a particular robot is assigned to be the leader, and all other robots are followers [50–52]. A predefined trajectory is to be tracked by the leader while the followers are supposed to follow the leader and keep a desired relative pose (distance and angle) from it. This approach is of particular interest because of its simplicity and modularity, specially for the cases where new robots are to join the formation [4]. Lack of feedback from the followers to the leader, however, is known to be a disadvantage of this approach. This is apparent when a follower is perturbed, and as a result the formation cannot be maintained due to the weak robustness [3]. Furthermore, the leader is a single point of failure for the formation [48]. Formation control for the leader-follower structure is extensively investigated in the control literature; see, e.g. [4], [50], [53–57].

1.6 Thesis Contributions

Formation control of mobile robots is studied extensively in the literature. However, most of the existing results rely on the relative distance and bearing of every pair of robots in the formation, for obtaining the control input. This leads to a system with complex formulation, especially when the number of robots in the formation is to be increased. In this

thesis, the control of a group of robots with a leader-follower structure is investigated. It is assumed that the robots have a chain configuration, and hence for controlling each robot only its relative distance and velocity with respect to its preceding robot is required. Using this technique, adding a new robot to the system will not require a new reformulation for obtaining the state-space representation of the system. The linear matrix inequality (LMI) technique is used for the stability analysis of the system. The stability of the formation with time-varying delay in the measurement signal is also studied and the dwell time between consecutive switches is obtained to ensure a prescribed steady-state performance. To the best of the author's knowledge, two problems of trajectory switching and delay in control input for the formation control system have never been studied concurrently in the literature.

The objectives of this thesis are listed below:

- Derive a control law for a single robot, so that system remains stable while tracking a trajectory
- Design a controller for the leader-follower formation problem so that the system is stable in the cases of perfect sensing and perfect sensing with input constraint
- Obtain upper bounds for the steady-state position and velocity errors in the presence of measurement noise
- Study the stability of system with time-varying delay in the measurement signal
- Derive a sufficient condition on the size of the time interval between consecutive switches by each robot so that the system remains exponentially convergent to a ball with a prescribed radius

1.7 Thesis Outline

This thesis is divided into five chapters that are described in the sequel.

In Chapter 2, the problem of trajectory tracking for a single WMR is studied. The state-space representation of the system is given, and a control input is then designed such that it stabilizes the trajectory tracking system. Input saturation is also addressed by imposing a constraint on the WMR control input. In addition, the steady-state performance of a single WMR is studied in the presence of measurement noise. Finally, some simulations are presented to demonstrate the efficiency of the developed results.

In Chapter 3, the formation control of a group of mobile robots with leader-follower structure is studied. Similar to Chapter 2, after deriving the state-space representation of the overall system, a control input is designed which guarantees the stability of the system in three cases of perfect sensing, perfect sensing with input constraint, and noisy measurements. Moreover, upper bounds for the steady-state position and velocity errors are obtained. Simulations are provided to validate the results obtained.

In Chapter 4, the stability of a platoon of WMRs with leader-follower structure is studied in the presence of input delay and switching in trajectories. An LMI-based approach is proposed to obtain the convergence properties for the tracking problem. Using the concepts of *dwell time* and *average dwell time* in switched systems, some bounds on the steady-state position and velocity errors are derived. Simulations are provided to show the effectiveness of the results.

Finally, Chapter 5 concludes the thesis with a general discussion highlighting the contributions of this research. Open problems and suggestions for future research work is also addressed in this chapter.

Table 1.1: Classification of sensors used in mobile robotics applications [1].

General classification (typical use)	Sensor Sensor System	PC or EC	A or P
Tactile Sensors	Contact switches, bumpers	EC	P
(detection of physical contact or	Optical barriers	EC	A
closeness; security switches)	Noncontact proximity sensor	EC	A
Wheel/motor sensors	Brush encoders	PC	P
(wheel/motor speed and position)	Potentiometers	PC	P
	Synchros, resolvers	PC	A
	Optical encoders	PC	A
	Magnetic encoders	PC	A
	Inductive encoders	PC	A
	Capacitive encoders	PC	A
Heading Sensors	Compass	EC	P
(orientation of the robot in relation to	Gyroscopes	PC	P
a fixed reference frame)	Inclinometers	EC	A/P
Ground-based beacons	GPS	EC	A
(localization in a fixed reference	Active optical or RF beacons	EC	A
frame)	Active ultrasonic beacons	EC	A
	Reflective beacons	EC	A
Active ranging	Reflectivity sensors	EC	A
(reflectivity, time-of-flight, and	Ultrasonic sensor	EC	A
geometric triangulation)	Laser rangefinder	EC	A
	Optical triangulation (1D)	EC	A
	Structured Light (2D)	EC	A
Motion/speed sensors	Doppler radar	EC	A
(speed relative to fixed or moving	Doppler sound	EC	A
objects)			
Vision-based sensors	CCD/CMOS camera(s)	EC	P
(visual ranging, whole-image analysis,	Visual ranging packages		
segmentation, object recognition)	Object tracking packages		

A, active; P, passive; P/A, passive/active; PC, proprioceptive; EC, exteroceptive.

Chapter 2

Trajectory Tracking by a Single Wheeled Mobile Robot

2.1 Introduction

Generally, there are two basic motion tasks [2] for wheeled mobile robots (Figure 2.1) as follows:

- Trajectory following: In this method, a point in the robot body is defined as the reference point. Given an initial configuration, robot's reference point is to track a geometric path in Cartesian space. To measure the tracking performance, an error function is defined. The error function has the same dimension as the input.

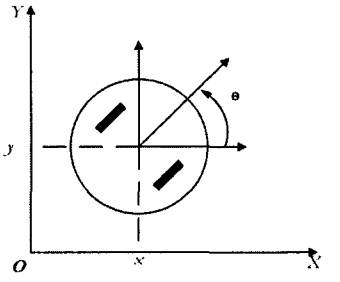

Figure 2.1: Wheeled mobile robot top view.

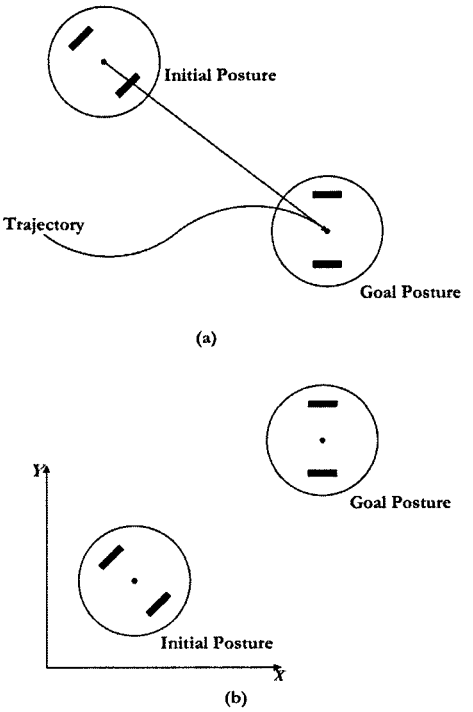

Figure 2.2: Wheeled mobile robot basic motion task: (a) trajectory tracking; (b) point-to-point motion [2].

Therefore, controlling the motion is easier than controlling the point-to-point motion which has less input commands (v and ω) than the variables (x, y, θ).

- Point-to-point motion: In this method, given an initial configuration for the mobile robot, a predefined configuration (as the mission objective) needs to be obtained. Moreover, the controller needs to be either discontinuous or time-varying due to non-holonomic constraint of the system. This is deduced from a necessary condition due to Brockett [8] which is: "for a smooth stabilization of a driftless regular system, it is necessary to have the same number of inputs as states" (see Figure 2.2).

The objective of this chapter is to control a single wheeled mobile robot (WMR), assuming there is no obstacle present in the environment. Trajectory following is used for the WMR motion.

This Chapter is organized as follows. The problem is formulated first and the main objective is presented in Section 2.2. Stability of the system will then be investigated in 3 different cases of perfect sensing, perfect sensing with input constraint, and perfect sensing with noisy measurement in Section 2.3. Simulations are provided in Section 2.4 to support the theoretical results obtained.

2.2 Problem Formulation

Let $z \in \mathbb{R}^n$ denote the set of all n-vectors of generalized coordinates for a wheeled mobile robot. This type of robot is often modeled as a single upright wheel. This model, which is also referred to as the unicycle model, is used to describe the behavior of the robot. The generalized coordinates for a unicycle are $z = (x, y, \theta)$, where (x, y) represents the Cartesian coordinates and θ is the angular orientation with respect to the x-axis in an inertial reference frame. The objective here is to control the robot in such a way that it follows a certain trajectory with a desired velocity. Let the inertial reference frame be centered at the origin O of the plane (see Figure 2.1), the differential equations describing the motion of the robot with respect to this frame are:

$$\begin{aligned} \dot{x} &= v\cos\theta \\ \dot{y} &= v\sin\theta \\ \dot{\theta} &= \omega \\ \dot{v} &= a \end{aligned} \tag{2.1}$$

where the acceleration a (which is directly related to force) is treated as the input variable. The error vector is subsequently defined as:

$$e = \begin{bmatrix} e_p \\ e_v \end{bmatrix} \tag{2.2}$$

where e_p and e_v are the position and velocity error of the robot, respectively, and are defined by:

$$e_p := \begin{bmatrix} e_{p_x} \\ e_{p_y} \end{bmatrix} = \begin{bmatrix} x - x_r \\ y - y_r \end{bmatrix} \tag{2.3}$$

and

$$e_v := \begin{bmatrix} e_{v_x} \\ e_{v_y} \end{bmatrix} = \begin{bmatrix} v\cos\theta - v_{x_r} \\ v\sin\theta - v_{y_r} \end{bmatrix} \tag{2.4}$$

where (x_r, y_r) is the reference value (set point) for the position of the robot, and (v_{x_r}, v_{y_r}) is the reference value for the velocity of the robot. It is assumed that the robot is equipped with the proper sensors to measure its relative position and velocity (with respect to the desired set points). Thus, the error vector e can be used in constructing the control input. Now, using equations (2.3) and (2.4) one can find:

$$\dot{e}_p = \begin{bmatrix} \dot{e}_{p_x} \\ \dot{e}_{p_y} \end{bmatrix} = \begin{bmatrix} v\cos\theta - v_{x_r} \\ v\sin\theta - v_{y_r} \end{bmatrix}$$

and similarly:

$$\dot{e}_v = \begin{bmatrix} \dot{e}_{v_x} \\ \dot{e}_{v_y} \end{bmatrix} = \begin{bmatrix} \dot{v}\cos\theta - v\dot{\theta}\sin\theta - a_{x_r} \\ \dot{v}\sin\theta + v\dot{\theta}\cos\theta - a_{y_r} \end{bmatrix}$$

where:

$$a_{x_r} = \frac{d}{dt}\left[v_{x_r}(t)\right]$$

and:

$$a_{y_r} = \frac{d}{dt}\left[v_{y_r}(t)\right]$$

By rewriting the above equations and using the relations (2.1), it can be shown that:

$$\dot{e}_v = \begin{bmatrix} \dot{e}_{v_x} \\ \dot{e}_{v_y} \end{bmatrix} = \begin{bmatrix} \cos\theta & -v\sin\theta \\ \sin\theta & v\cos\theta \end{bmatrix} \begin{bmatrix} a \\ \omega \end{bmatrix} - \begin{bmatrix} a_{x_r} \\ a_{y_r} \end{bmatrix} \tag{2.5}$$

Define:

$$\begin{bmatrix} u_1 \\ u_2 \end{bmatrix} = \begin{bmatrix} \cos\theta & -v\sin\theta \\ \sin\theta & v\cos\theta \end{bmatrix} \begin{bmatrix} a \\ \omega \end{bmatrix}$$

Hence, (2.5) can be expressed as:

$$\begin{bmatrix} \dot{e}_{v_x} \\ \dot{e}_{v_y} \end{bmatrix} = \begin{bmatrix} u_1 \\ u_2 \end{bmatrix} - \begin{bmatrix} a_{x_r} \\ a_{y_r} \end{bmatrix}$$

Combining the differential equations for the position and velocity errors, the state space representation of the system can be written as:

$$\begin{bmatrix} \dot{e}_{p_x} \\ \dot{e}_{p_y} \\ \dot{e}_{v_x} \\ \dot{e}_{v_y} \end{bmatrix} = \underbrace{\begin{bmatrix} 0 & 0 & 1 & 0 \\ 0 & 0 & 0 & 1 \\ 0 & 0 & 0 & 0 \\ 0 & 0 & 0 & 0 \end{bmatrix}}_{A} \begin{bmatrix} e_{p_x} \\ e_{p_y} \\ e_{v_x} \\ e_{v_y} \end{bmatrix} + \underbrace{\begin{bmatrix} 0 & 0 \\ 0 & 0 \\ 1 & 0 \\ 0 & 1 \end{bmatrix}}_{B} \begin{bmatrix} u_1 \\ u_2 \end{bmatrix} - \underbrace{\begin{bmatrix} 0 & 0 \\ 0 & 0 \\ 1 & 0 \\ 0 & 1 \end{bmatrix}}_{B} \begin{bmatrix} a_{x_r} \\ a_{y_r} \end{bmatrix}$$

or equivalently:

$$\dot{e} = Ae + Bu - Ba_r \tag{2.6}$$

where a_r is the reference value for the acceleration of the robot in the x and y directions, and is expressed as:

$$a_r := \begin{bmatrix} a_{x_r} \\ a_{y_r} \end{bmatrix}$$

It is desired to design a control law of the following form:

$$u = Ke + a_r := a + a_r \tag{2.7}$$

to regulate the error defined by (2.2), where $K \in \mathbb{R}^{2\times 4}$ is a constant matrix.

2.3 Main Results

2.3.1 Perfect Sensing without Input Constraint

In this section, it is desired to investigate the stability of system (2.6) under the controller of the form (2.7), assuming that no error exists in sensor measurements.

Theorem 2.1. *Consider a mobile robot following a desired trajectory, where the error dynamics of the robot is governed by (2.6). Given $\alpha > 0$, suppose that there exist $R > 0$ and S satisfying the following LMI:*

$$RA^T + AR + S^T B^T + BS + \alpha R < 0 \tag{2.8}$$

Apply the controller (2.7) with $K = SR^{-1}$ to the robot; then $\|e(t)\|$ is exponentially decaying (where $\|.\|$ denotes the 2-norm).

Proof: The error dynamics (2.6) under controller (2.7) can be described by:

$$\dot{e} = (A + BK)e$$

Let $V = e^T Pe$; then

$$\dot{V} + \alpha V = 2e^T P(A + BK)e + \alpha e^T Pe$$

Now, if:

$$(A + BK)^T P + P(A + BK) + \alpha P < 0 \tag{2.9}$$

then it follows that:

$$\dot{V} + \alpha V < 0 \tag{2.10}$$

which implies that $V(t)$ and $e(t)$ are also exponentially decaying. Choose $P = R^{-1}$ and $K = SP$; then (2.9) becomes equivalent to (2.8). This completes the proof. ■

2.3.2 Perfect Sensing with Input Constraint

Theorem 2.2. *Consider the system described in Theorem 2.1 and let* $\mu_1 = \max||e_{p_x}|| = \max||e_{p_y}||$ *and* $\mu_2 = \max||e_{v_x}|| = \max||e_{v_y}||$. *Given the design parameters* $\alpha > 0$, $\eta > 0$, *solve the following LMIs*

$$RA^T + AR + S^T B^T + BS + \alpha R < 0 \tag{2.11}$$

and

$$\begin{bmatrix} \eta^2 R & S^T \\ S & I_2 \end{bmatrix} > 0 \tag{2.12}$$

$$R > 4 \begin{bmatrix} \mu_1{}^2 I_2 & 0 \\ 0 & \mu_2{}^2 I_2 \end{bmatrix} \tag{2.13}$$

where I_2 *is the* 2×2 *identity matrix. Assume the problem has a feasible solution; then:*

i) If the controller (2.7) with $K = SR^{-1}$ *is applied to the robot, then* $\|e(t)\|$ *is exponentially decaying, and*

ii) $||u|| < \eta$.

Proof: According to Theorem 2.1, (2.11) implies that $\|e(t)\|$ is exponentially decaying. Multiplying (2.12) by $\begin{bmatrix} R^{-1} & 0 \\ 0 & I_2 \end{bmatrix} > 0$ from left and right yields:

$$\begin{bmatrix} \eta^2 R^{-1} & K^T \\ K & I_2 \end{bmatrix} > 0 \tag{2.14}$$

Using the *Schur complement* theorem [58] and choosing $P = R^{-1}$, inequality (2.14) can be expressed as:

$$K^T K \leq \eta^2 P \tag{2.15}$$

On the other hand:

$$\|Ke\|^2 = e^T K^T K e < \eta^2 e^T P e \tag{2.16}$$

To make $\|u\| < \eta$, it is sufficient to have:

$$e^T P e < 1 \tag{2.17}$$

for all $t > t_0$. Consider the following ellipsoid ε centered at the origin:

$$\varepsilon = \{e \in R^n | e^T P e < 1\}$$

Since $\|e(t)\|$ is exponentially decaying, ε is an invariant ellipsoid [58]. Thus, if:

$$e^T(t_0) P e(t_0) < 1 \tag{2.18}$$

then (2.17) is satisfied. Choose R such that:

$$R^{-1} < \frac{1}{4} \begin{bmatrix} {\mu_1}^{-2} I_2 & 0 \\ 0 & {\mu_2}^{-2} I_2 \end{bmatrix}$$

to obtain:

$$e(t_0)^T R^{-1} e(t_0) < \frac{1}{4} \left[{\mu_1}^{-2} \|e_{p_x}(t_0)\|^2 + {\mu_1}^{-2} \|e_{p_y}(t_0)\|^2 \right.$$
$$\left. + {\mu_2}^{-2} \|e_{v_x}(t_0)\|^2 + {\mu_2}^{-2} \|e_{v_y}(t_0)\|^2 \right] < 1 \tag{2.19}$$

which yields (2.18). The proof follows from the above inequalities. ■

2.3.3 Noisy Measurements

In order to take into account the effect of measurement noise on the robot's motion, the control law (2.7) is modified as:

$$u = K\tilde{e} + a_r \tag{2.20}$$

where $\tilde{e} = e + \delta_e$, and δ_e is the measurement noise which is assumed to have a known bound represented by:

$$\Delta_e := \max_{t>t_0} ||\delta_e||^2$$

In this subsection, an upper bound on the steady-state error is obtained and an algorithm is proposed to design K such that this upper bound is minimized.

Lemma 2.1. *Given a positive scalar α, let the following inequality hold:*

$$\dot{V} + \alpha V - b{\delta_e}^T Q \delta_e < 0 \tag{2.21}$$

where b is a positive constant and Q is a symmetric positive definite matrix. Then:

$$V(\infty) < \frac{b}{\alpha} \max_{t>t_0} [{\delta_e}^T(t) Q \delta_e(t)] \tag{2.22}$$

Proof: Multiply (2.21) by $e^{\alpha t}$, to obtain:

$$\frac{d}{dt}[e^{\alpha t} V] < b\delta_e(t)^T Q \delta_e(t) e^{\alpha t}$$

Integrating from t_0 to t yields:

$$e^{\alpha t} V(t) - e^{\alpha t_0} V(t_0) < \int_{t_0}^{t} [b{\delta_e}^T(\tau) Q \delta_e(\tau)] e^{\alpha \tau} d\tau$$

Multiplying again by $e^{-\alpha t}$ results in:

$$V(t) < \frac{b}{\alpha} \max_{t>t_0} [\delta_e{}^T(t) Q \delta_e(t)(e^{\alpha t} - e^{\alpha t_0})] e^{-\alpha t} + e^{-\alpha(t-t_0)} V(t_0)$$

Now, (2.22) is obtained for $t \to \infty$. ■

Consider now the system described in Theorem 2.1. Assume R has a lower bound R_l and an upper bound R_r given below:

$$R_l = \begin{bmatrix} \beta_1 & 0 & 0 & 0 \\ 0 & \beta_1 & 0 & 0 \\ 0 & 0 & \beta_2 & 0 \\ 0 & 0 & 0 & \beta_2 \end{bmatrix} \tag{2.23a}$$

$$R_r = \begin{bmatrix} \gamma_1 & 0 & 0 & 0 \\ 0 & \gamma_1 & 0 & 0 \\ 0 & 0 & \frac{1}{\varepsilon_0} & 0 \\ 0 & 0 & 0 & \frac{1}{\varepsilon_0} \end{bmatrix} \tag{2.23b}$$

where β_1 and β_2 are weighting factors corresponding to the position and velocity error, respectively. Furthermore, $\gamma_1 > 0$ is another weighting factor, and ε_0 is a sufficiently small positive number.

Let the design parameters $\alpha > 0$ and $b_f > 0$ be given. For any scalar $0 < b < b_f$,

solve the following optimization problem:

$$\min \ [\Omega_{\beta_1}\beta_1 + \Omega_{\beta_2}\beta_2 + \Omega_{\gamma_1}\gamma_1]$$

subject to

$$\begin{bmatrix} RA^T + AR + S^TB^T + BS + \alpha R & BS \\ S^TB^T & -bR \end{bmatrix} < 0$$

and

$$R_l < R < R_r$$

w.r.t.

$$\beta_1 > 0,\ \beta_2 > 0,\ \gamma_1 > 0$$

where Ω_{β_1}, $\Omega_{\beta_2} < 0$ and $\Omega_{\gamma_1} > 0$, are weighting coefficients. It is to be noted that the matrix constraint in the above optimization problem is in the form of LMI. If the above problem is feasible, calculate:

$$\bar{e_p}^2 = \frac{b\gamma_1}{\alpha\beta_1}\Delta_{e_p} + \frac{b\gamma_1}{\alpha\beta_2}\Delta_{e_v}$$

where $\Delta_{e_p} := \max_{t>t_0} ||\delta_{e_p}||^2$ and $\Delta_{e_v} := \max_{t>t_0} ||\delta_{e_v}||^2$. Define also

$$\bar{e}_{p,\min} := \min_{0<b<b_f} \bar{e_p}$$

In the next theorem, upper bounds on the steady state position error and steady-state velocity error are obtained.

Theorem 2.3. *If the controller (2.20) is applied to the robot described by (2.1) with* $K = SR^{-1}$, *where S and R are given in the above optimization problem, then:*

i) $\|e(t)\|$ *is exponentially decaying for* $\Delta_e = 0$.

ii) $\lim_{t\to\infty} ||e_p|| < \bar{e}_{p,\min}$.

Proof: The closed-loop system under controller (2.20) can be represented by:

$$\dot{e} = (A + BK)e + BK\delta_e \tag{2.24}$$

Let $V(t)$ in (2.21) be equal to $e^T R^{-1} e$, and choose $Q = R^{-1}$. It can be shown (similarly to the proof of Theorem 2.1) that:

$$\begin{aligned} \dot{V} + \alpha V - b{\delta_e}^T Q \delta_e < {} & e^T A^T R^{-1} e + e^T R^{-1} A e + e^T K^T B^T R^{-1} e + {\delta_e}^T K^T B^T R^{-1} e \\ & + e^T R^{-1} B K e + e^T R^{-1} B K \delta_e + \alpha e^T R^{-1} e - b{\delta_e}^T R^{-1} \delta_e \end{aligned} \tag{2.25}$$

Let the right-hand side expression in (2.25) be negative. This condition can now be rewritten in the following matrix form:

$$\begin{bmatrix} e^T & {\delta_e}^T \end{bmatrix}^T \begin{bmatrix} A^T R^{-1} + R^{-1} A + K^T B^T R^{-1} + R^{-1} B K + \alpha R^{-1} & R^{-1} B K \\ K^T B^T R^{-1} & -bR^{-1} \end{bmatrix} \begin{bmatrix} e \\ \delta_e \end{bmatrix} < 0 \tag{2.26}$$

Relation (2.26) holds for every e and δ_e ($[e \;\; \delta_e] \neq 0$) if and only if the following inequality is satisfied:

$$\begin{bmatrix} A^T R^{-1} + R^{-1} A + K^T B^T R^{-1} + R^{-1} B K + \alpha R^{-1} & R^{-1} B K \\ K^T B^T R^{-1} & -bR^{-1} \end{bmatrix} < 0 \tag{2.27}$$

Pre and post-multiplying (2.27) by $\begin{bmatrix} R & 0 \\ 0 & R \end{bmatrix}$ and defining $KR = S$ leads to:

$$\begin{bmatrix} RA^T + AR + S^T B^T + BS + \alpha R & BS \\ S^T B^T & -bR \end{bmatrix} < 0 \tag{2.28}$$

Now, if (2.28) holds, it is concluded from Lemma 2.1 that:

$$e(\infty)^T R^{-1} e(\infty) < \frac{b}{\alpha} \max_{t>t_0} [\delta_e{}^T(t) R^{-1} \delta_e(t)] \tag{2.29}$$

In order to find an upper bound for the steady-state error, one can use (2.23a) to obtain:

$$\begin{aligned} \delta_e{}^T(t) R^{-1} \delta_e(t) &< \begin{bmatrix} \delta_{e_p} & \delta_{e_v} \end{bmatrix} \begin{bmatrix} \frac{1}{\beta_1} & 0 & 0 & 0 \\ 0 & \frac{1}{\beta_1} & 0 & 0 \\ 0 & 0 & \frac{1}{\beta_2} & 0 \\ 0 & 0 & 0 & \frac{1}{\beta_2} \end{bmatrix} \begin{bmatrix} \delta_{e_p} \\ \delta_{e_v} \end{bmatrix} \\ &\leq \frac{1}{\beta_1} ||\delta_{e_p}||^2 + \frac{1}{\beta_2} ||\delta_{e_v}||^2 \end{aligned} \tag{2.30}$$

On the other hand, the following inequality results from (2.23b) for the lower bound:

$$\begin{aligned} e^T(t) R^{-1} e(t) &> \begin{bmatrix} e_p & e_v \end{bmatrix} \begin{bmatrix} \frac{1}{\gamma_1} & 0 & 0 & 0 \\ 0 & \frac{1}{\gamma_1} & 0 & 0 \\ 0 & 0 & \varepsilon_0 & 0 \\ 0 & 0 & 0 & \varepsilon_0 \end{bmatrix} \begin{bmatrix} e_p \\ e_v \end{bmatrix} \\ &\geq \frac{1}{\gamma_1} ||e_p||^2 + \varepsilon_0 ||e_v||^2 \end{aligned}$$

or equivalently:

$$\frac{1}{\gamma_1} ||e_p||^2 \leq \frac{1}{\gamma_1} ||e_p||^2 + \varepsilon_0 ||e_v||^2 \leq e^T(t) R^{-1} e(t) \tag{2.31}$$

Thus, using (2.29), it follows that:

$$\frac{1}{\gamma_1} ||e_p(\infty)||^2 < \frac{b}{\alpha} \max_{t>t_0} [\delta_e{}^T(t) R^{-1} \delta_e(t)] \tag{2.32}$$

Substituting the upper limits for the position and velocity measured noise from (2.30) and

(2.32), an upper bound on the steady-state position error is obtained as follows:

$$||e_p(\infty)||^2 < \frac{b\gamma_1}{\alpha\beta_1}\Delta_{e_p} + \frac{b\gamma_1}{\alpha\beta_2}\Delta_{e_v} \tag{2.33}$$

The parameters β_1, β_2 and γ_1 can be regarded as the free variables of a minimization problem. In addition, note that a necessary condition for (2.28) to hold is:

$$RA^T + AR + S^T B^T + BS + \alpha R < 0$$

which implies that $e(t)$ is exponentially decaying for $\Delta_e = 0$, according to Theorem 2.1. ■

Remark 2.1. *A similar approach can be used to obtain an upper bound on the steady-state velocity error. To this end, R_r needs to be replaced by:*

$$R_r = \begin{bmatrix} \frac{1}{\varepsilon_0} & 0 & 0 & 0 \\ 0 & \frac{1}{\varepsilon_0} & 0 & 0 \\ 0 & 0 & \gamma_1 & 0 \\ 0 & 0 & 0 & \gamma_1 \end{bmatrix}$$

which leads to the following upper bound:

$$||e_v(\infty)||^2 < \frac{b\gamma_1}{\alpha\beta_1}\Delta_{e_p} + \frac{b\gamma_1}{\alpha\beta_2}\Delta_{e_v}$$

Remark 2.2. *It is to be noted that the condition (2.21) becomes relaxed when the measurement error δ_e is larger. Thus, smaller values could be found for the ratios γ_1/β_1 and γ_1/β_2 in such cases. This concludes that the upper bound introduced in (2.33) is not directly proportional to Δ_{e_p} and Δ_{e_v}.*

2.4 Simulation Results

In Example 2.1 the results obtained for the tracking problem in the presence of input constraint are examined by simulations. Example 2.2 is presented to verify the results associated with the maximum bound on steady-state error.

Example 2.1. *Consider a WMR, and let the desired trajectory to be followed by the robot be a path given by,*

a) $x_r = 2\cos 0.025t, \quad y_r = 2\sin 0.025t$ *(circular trajectory)*

b) $x_r = \sin 0.1t, \quad y_r = \sin 0.2t$ *(eight-shaped trajectory)*

It is desired to obtain a control input of the form (2.7) in which the magnitude of a *is less than* η *at all times, while the tracking objective described above is achieved.*

Assume that the experiment is to be performed in a 4×4 m *environment; hence,* $\max||e_{p_x}|| = \max||e_{p_y}|| = \mu_1 = 4$. *Furthermore, let the maximum speed of the robot be* 0.3 m/sec, *i.e.,* $\max||e_{v_x}|| = \max||e_{v_y}|| = \mu_2 = 0.3$. *Let also* η=0.04*; one can then use Theorem 2.2 with* $\alpha = 0.04$ *and* $\varepsilon_0 = 2 \times 10^{-9}$ *to obtain the gain matrix K in (2.7) as:*

$$K = \begin{bmatrix} -0.0007 & 0 & -0.0469 & 0 \\ 0 & -0.0007 & 0 & -0.0469 \end{bmatrix} \tag{2.34}$$

- *Case (a):*

  In Figure 2.3, the robot's trajectory in the x-axis is compared with the desired circular trajectory. A similar comparison is made in the y direction in Figure 2.4. These two figures demonstrate that the position tracking objective is achieved here.

  Figure 2.5 shows that the velocity regulation error e_v *approaches zero in both x and y directions. Figure 2.6 shows the trajectory of the robot moving toward the circular path from its initial position (1.9,0.1). The norm of the control input for the*

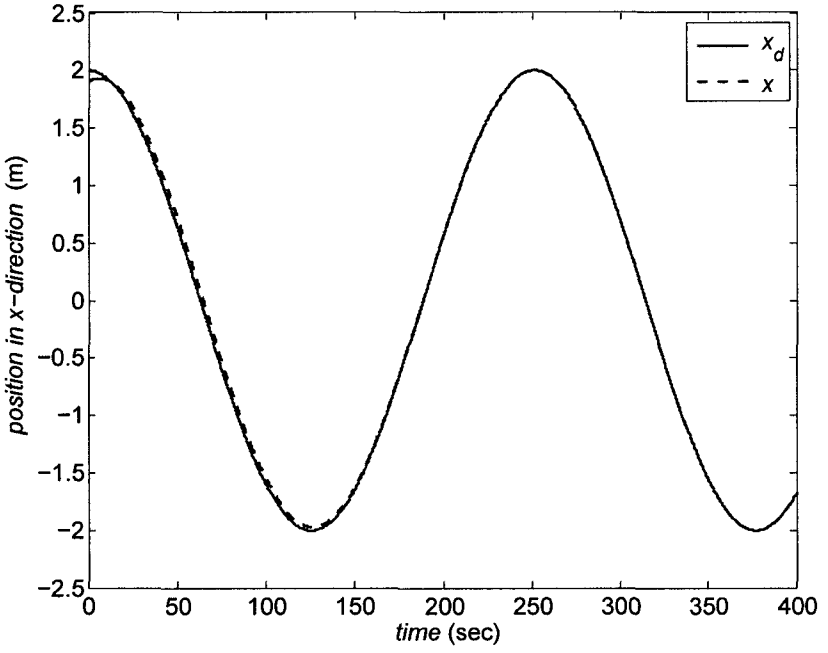

Figure 2.3: The robot's trajectory tracking along the x-axis for the circular reference signal in Example 2.1(a).

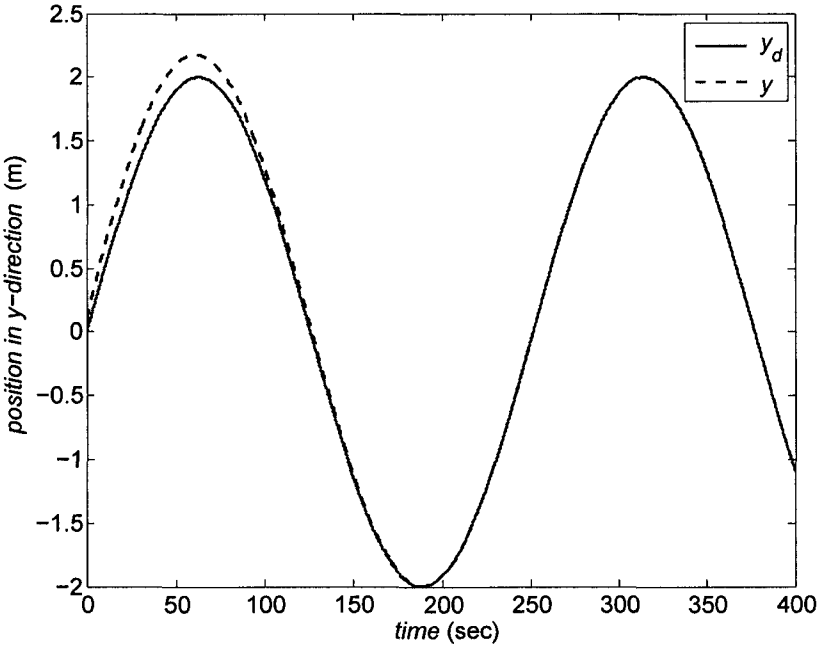

Figure 2.4: The robot's trajectory tracking along the y-axis for the circular reference signal in Example 2.1(a).

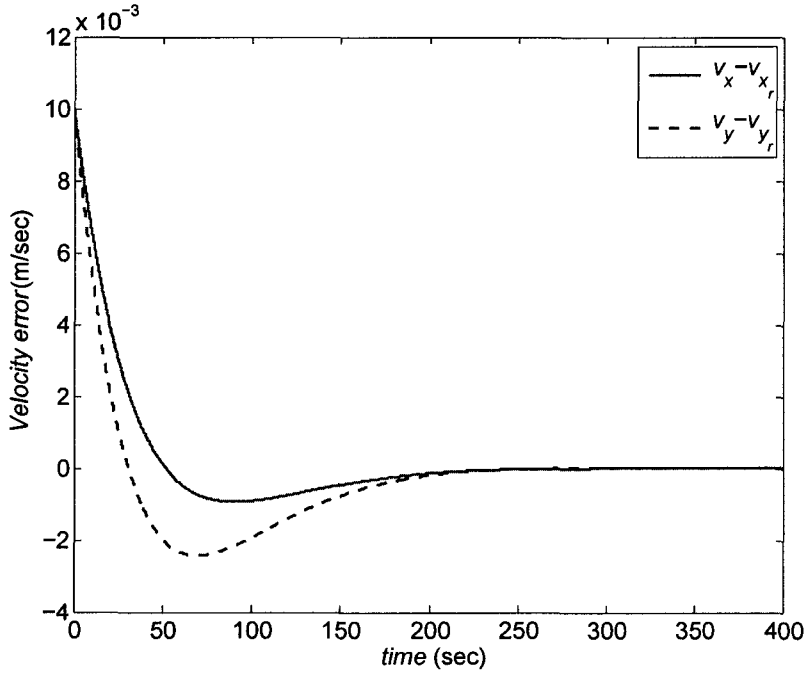

Figure 2.5: The velocity error of the robot for the circular reference signal in Example 2.1(a).

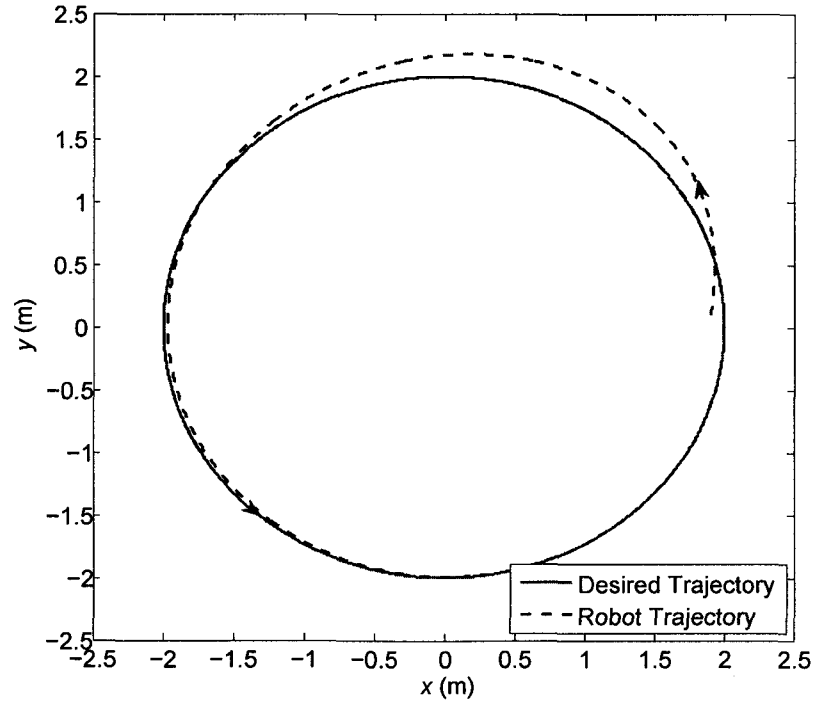

Figure 2.6: The robot's trajectory in the 2-D plane for the circular reference signal in Example 2.1(a).

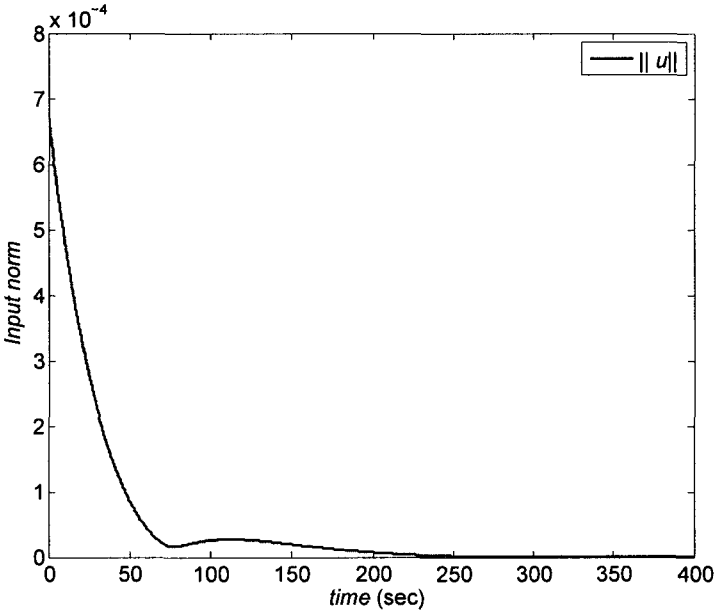

Figure 2.7: The norm of the control input ($||u||$) for the circular reference signal in Example 2.1(a).

robot is depicted in Figure 2.7, which confirms that the input constraint is satisfied.

- *Case (b):*

  In Figure 2.8, the robot's trajectory in the x-axis is compared with the desired eight-shaped trajectory. A similar comparison is made in the y direction in Figure 2.9. Again, the simulations demonstrate that the tracking objective is achieved. Figure 2.10 shows that the velocity regulation error e_v approaches zero in both directions x and y. Figure 2.11 shows the trajectory of the robot moving toward the eight-shaped path from its initial position (-0.1,0.1). The norm of the control input for the robot is depicted in Figure 2.12, which shows that the input constraint is fulfilled.

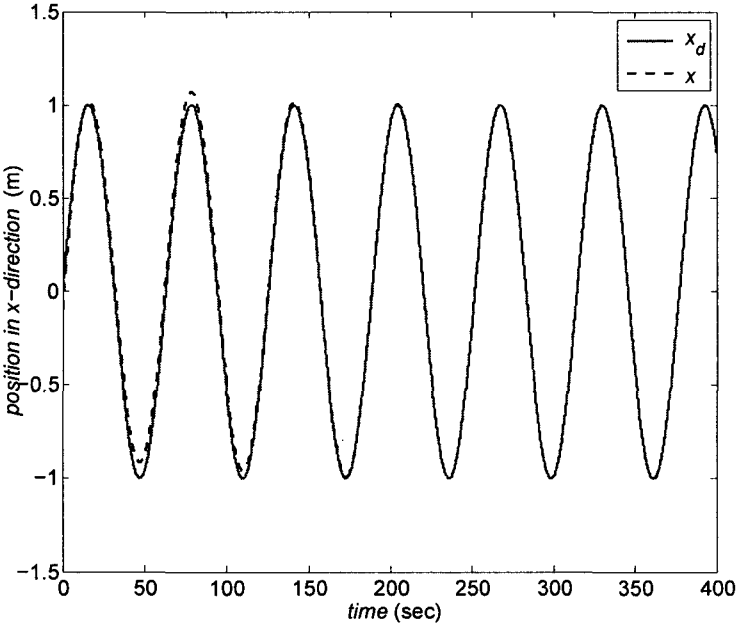

Figure 2.8: The robot's trajectory tracking along the x-axis for the eight-shaped reference signal in Example 2.1(b).

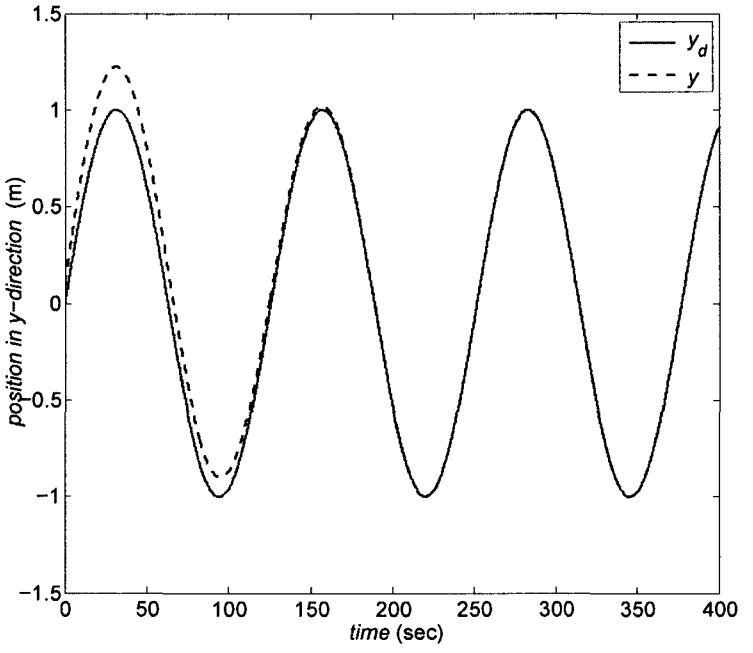

Figure 2.9: The robot's trajectory tracking along the y-axis for the eight-shaped reference signal in Example 2.1(b).

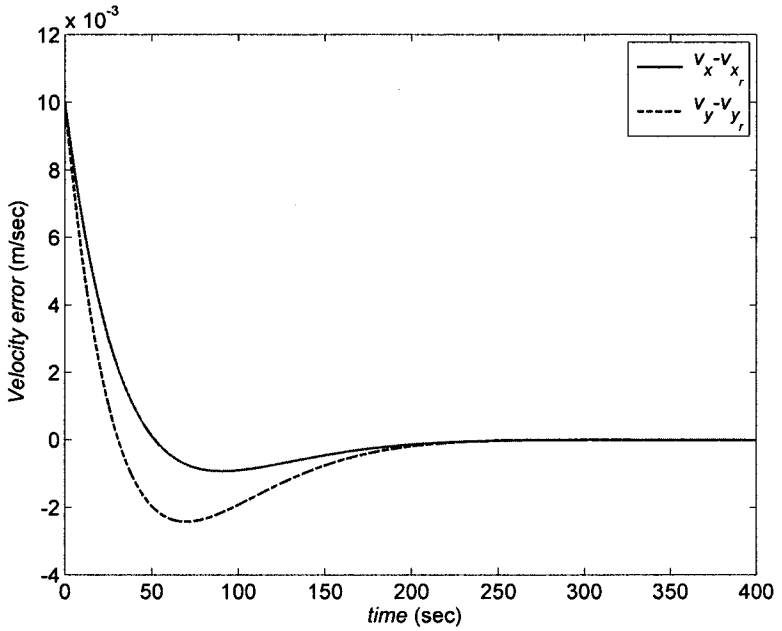

Figure 2.10: The velocity error of the robot for the eight-shaped reference signal in Example 2.1(b).

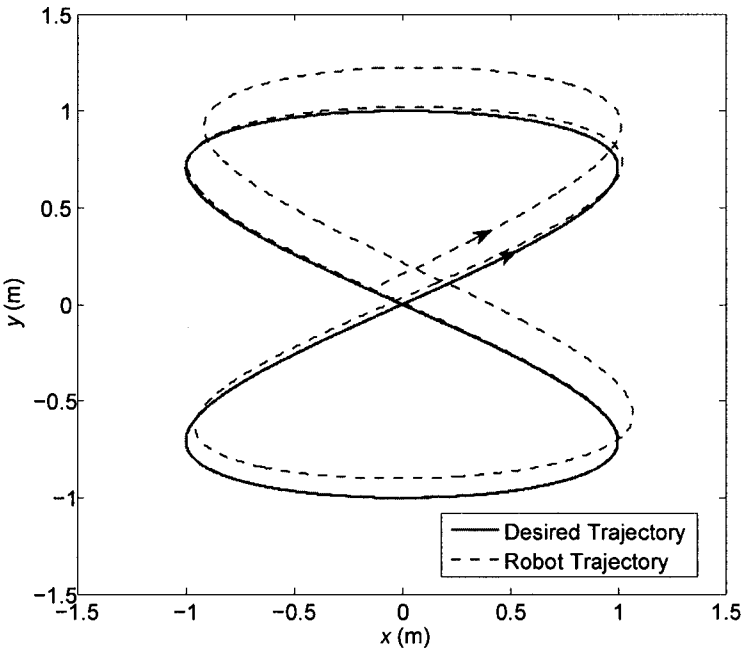

Figure 2.11: The robot's trajectory in the 2-D plane for the eight-shaped reference signal in Example 2.1(b).

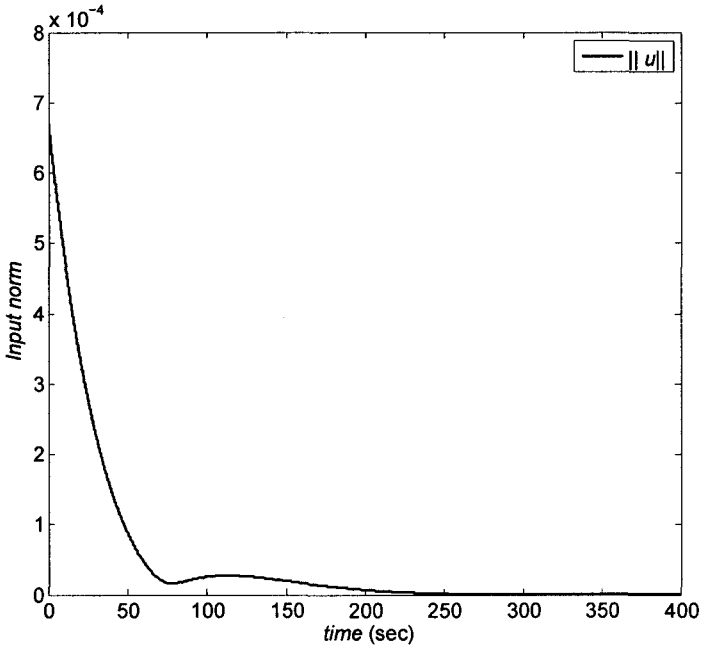

Figure 2.12: The norm of the control input ($||u||$) for the eight-shaped reference signal in Example 2.1(b).

Example 2.2. *In this Example, it is assumed that the robot is to follow a linear path (ramp reference tracking) is characterized by:*

$$x_r = y_r = 0.4t \tag{2.35}$$

Let $\alpha = 0.04$, $\Omega_{\beta_1} = -1$, $\Omega_{\beta_2} = -2$, *and* $\Omega_{\gamma_1} = 1$. *Assume that the measurement noise is a random process which is uniformly distributed in the intervals* $(0, 2 \times 10^{-5})$ *and* $(0, 10^{-3})$ *for position and velocity measurements, respectively. Using Theorem 2.3 with* $b = 1.55$, *the gain matrix given below is obtained:*

$$K = \begin{bmatrix} -1.6724 & 0 & -0.7615 & 0 \\ 0 & -1.6724 & 0 & -0.7615 \end{bmatrix}$$

It also results from Theorem 2.3 that an upper bound for the steady-state position error is 9.7×10^{-3}. *The value of the maximum error obtained by simulation is approximately*

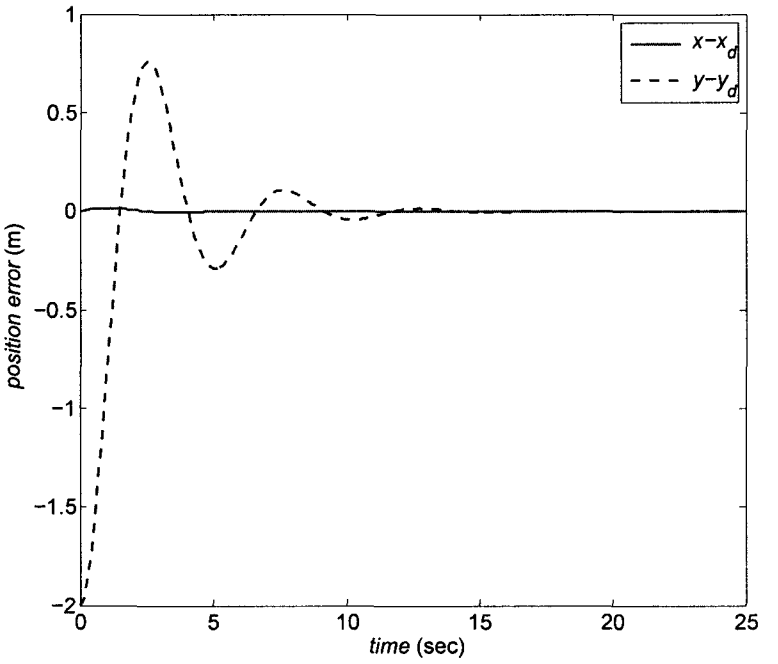

Figure 2.13: The position error along the x and y axes for the linear trajectory tracking of Example 2.2.

equal to 5×10^{-3}, *which complies with the above result. Figure 2.13 depicts the relative position of robot with respect to its desired value in both x and y directions. The velocity errors of the robot along the x and y axes are plotted in Figure 2.14, which both converge to zero. The planar motion of the formation is sketched in Figure 2.15.*

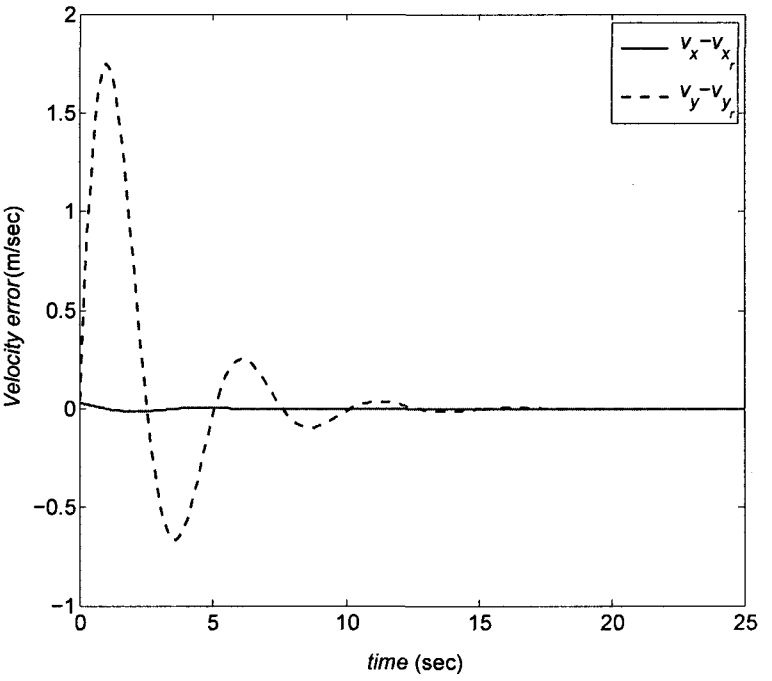

Figure 2.14: The velocity error for the linear trajectory tracking of Example 2.2.

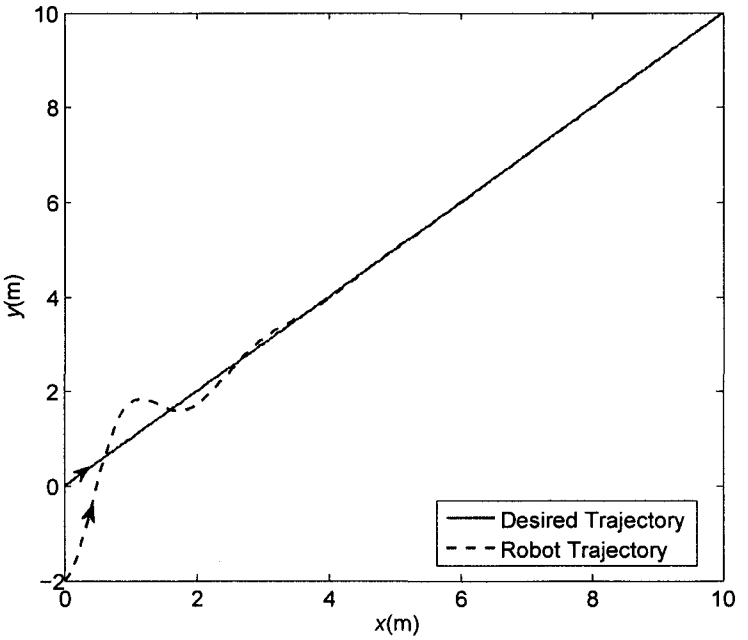

Figure 2.15: the robot's trajectory in the 2-D plane for the linear trajectory tracking of Example 2.2.

Chapter 3

Formation Control of a Platoon of Wheeled Mobile Robots Subject to Input Constraint and Measurement Noise

3.1 Introduction

In this chapter, the problem of controlling a group of mobile robots following a trajectory while maintaining their formation intact is considered. The control design is carried out for the case of unicycle kinematics, which is the most common among wheeled mobile robots (WMR). It is assumed that every robot except the leader and the one located at the end of each platoon may potentially be a follower with respect to the one immediately in front of it, or a leader with respect to the one behind it (see Figure 3.1). The desired relative position of each follower with respect to its corresponding leader is assumed to be known by that follower. It is assumed also that each follower is capable of sensing its relative distance and relative velocity with respect to its preceding robot.

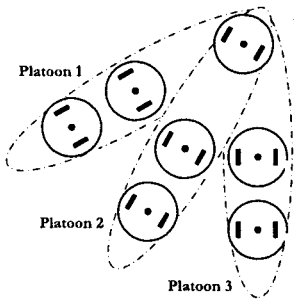

Figure 3.1: Platoon of Mobile Robots.

First, the stability of the system is investigated in the case of perfect sensing. A feedback control law is subsequently proposed to satisfy the design specifications. The impact of measurement noise on the followers' motion is then studied, and a control design methodology is introduced using linear matrix inequalities (LMI) to minimize the effect of noise.

This chapter is organized as follows. The problem is formulated in Section 3.1, where the main objectives of the work are also presented. In Section 3.2, control strategies are proposed which take the input constraint into account, and suppress the effect of measurement noise. Section 3.3 presents simulations to validate the theoretical results obtained in this chapter.

3.2 Problem Formulation

Let $z \in \mathbb{R}^n$ denote the set of all n-vectors of generalized coordinates for a WMR. The generalized coordinates for a unicycle are $z = (x, y, \theta)$, where (x, y) represents the Cartesian coordinates and θ is the angular orientation with respect to the x-axis in an inertial reference frame. It is desired to control the followers in such a way that they follow the leader with a desired accuracy, while the leader follows an unknown trajectory. Let the inertial reference frame be centered at the origin O of the plane (see Figure 2.1), the differential equations describing the motion of the i-th robot, $i \in \mathbf{n} := \{1, ..., n\}$, with respect to this

frame are:

$$\begin{aligned} \dot{x}^i &= v^i \cos\theta^i \\ \dot{y}^i &= v^i \sin\theta^i \\ \dot{\theta}^i &= \omega^i \\ \dot{v}^i &= a^i \end{aligned} \tag{3.1}$$

where the acceleration a is the input variable. By assumption, robot 1 is the leader, and its dynamic equations is expressed as:

$$\begin{aligned} \dot{x}^l &= v^l \cos\theta^l \\ \dot{y}^l &= v^l \sin\theta^l \\ \dot{\theta}^l &= \omega^l \\ \dot{v}^l &= a^l \end{aligned} \tag{3.2}$$

The error vector for the i-th follower, $i \in \{2,...,n\}$, is subsequently defined as:

$$e^i = \begin{bmatrix} e_p^i \\ e_v^i \end{bmatrix} \tag{3.3}$$

where e_p^i and e_v^i are position and velocity error of the i-th follower, respectively, and are defined by:

$$e_p^i := \begin{bmatrix} e_{p_x}^i \\ e_{p_y}^i \end{bmatrix} = \begin{bmatrix} x^i - x^{i-1} - d_x^i(t) \\ y^i - y^{i-1} - d_y^i(t) \end{bmatrix} \tag{3.4}$$

and

$$e_v^i := \begin{bmatrix} e_{v_x}^i \\ e_{v_y}^i \end{bmatrix} = \begin{bmatrix} \dot{x}^i - \dot{x}^{i-1} \\ \dot{y}^i - \dot{y}^{i-1} \end{bmatrix} \tag{3.5}$$

where $d_x^i(t)$ and $d_y^i(t)$ represent the desired relative position between the i-th and $(i-1)$-th robots in the platoon in the x and y directions, respectively. The objective here is to make the position and velocity errors as close as possible to zero. It is to be noted that if $e_{v_x}^i$ and

$e^i_{v_y}$ tend to zero, then $\theta^i \to \theta^{i-1}$. This means that if the velocity error approaches zero by time, then the orientation alignment of all robots in the platoon is guaranteed in the steady state.

Assumption 3.1. *The desired relative positions $d^i_x(t)$ and $d^i_y(t)$ are either constant or the outputs of an autonomous system represented by*

$$\dot{q}(t) = \Gamma q(t)$$
$$d^i_x(t) = \Pi_x q(t)$$
$$d^i_y(t) = \Pi_y q(t)$$

where $q \in \mathbb{R}^K$. Note that all the eigenvalues of the Γ lie in the open left half-plane except one which is located in the origin. Denote with $-\lambda$ the rightmost non-zero eigenvalues of Γ.

It is supposed that each follower is equipped with the proper sensors to measure its relative position and velocity (with respect to its preceding robot). Thus, the error vector e^i can be used in constructing the control input. Now, using equations (3.4) and (3.5), one can write:

$$\dot{e}^i_p = \begin{bmatrix} \dot{e}^i_{p_x} \\ \dot{e}^i_{p_y} \end{bmatrix} = \begin{bmatrix} e^i_{v_x} - \dot{d}^i_x(t) \\ e^i_{v_y} - \dot{d}^i_y(t) \end{bmatrix}$$

and similarly:

$$\dot{e}^i_v = \begin{bmatrix} \dot{e}^i_{v_x} \\ \dot{e}^i_{v_y} \end{bmatrix} = \begin{bmatrix} \dot{v}^i \cos\theta^i - v^i \dot{\theta}^i \sin\theta^i - \ddot{x}^{i-1} \\ \dot{v}^i \sin\theta^i + v^i \dot{\theta}^i \cos\theta^i - \ddot{y}^{i-1} \end{bmatrix}$$

By rewriting the above equations and using the relations $\dot{\theta}^i = \omega$ and $\dot{v}^i = a^i$, it can be shown that:

$$\dot{e}^i_v = \begin{bmatrix} \dot{e}^i_{v_x} \\ \dot{e}^i_{v_y} \end{bmatrix} = \begin{bmatrix} \cos\theta^i & -v^i \sin\theta^i \\ \sin\theta^i & v^i \cos\theta^i \end{bmatrix} \begin{bmatrix} a^i \\ \omega^i \end{bmatrix} - \begin{bmatrix} \ddot{x}^{i-1} \\ \ddot{y}^{i-1} \end{bmatrix}$$

Define:

$$\begin{bmatrix} u_1^i \\ u_2^i \end{bmatrix} = \begin{bmatrix} \cos\theta^i & -v^i \sin\theta^i \\ \sin\theta^i & v^i \cos\theta^i \end{bmatrix} \begin{bmatrix} a^i \\ \omega^i \end{bmatrix}$$

Then:

$$\begin{bmatrix} \dot{e}_{v_x}^i \\ \dot{e}_{v_y}^i \end{bmatrix} = \begin{bmatrix} u_1^i \\ u_2^i \end{bmatrix} - \begin{bmatrix} \ddot{x}^{i-1} \\ \ddot{y}^{i-1} \end{bmatrix}$$

Combining the two equations, the error dynamics can be expressed as:

$$\begin{bmatrix} \dot{e}_{p_x}^i \\ \dot{e}_{p_y}^i \\ \dot{e}_{v_x}^i \\ \dot{e}_{v_y}^i \end{bmatrix} = \underbrace{\begin{bmatrix} 0 & 0 & 1 & 0 \\ 0 & 0 & 0 & 1 \\ 0 & 0 & 0 & 0 \\ 0 & 0 & 0 & 0 \end{bmatrix}}_{A} \begin{bmatrix} e_{p_x}^i \\ e_{p_y}^i \\ e_{v_x}^i \\ e_{v_y}^i \end{bmatrix} + \underbrace{\begin{bmatrix} 0 & 0 \\ 0 & 0 \\ 1 & 0 \\ 0 & 1 \end{bmatrix}}_{B} \begin{bmatrix} u_1^i \\ u_2^i \end{bmatrix} - \underbrace{\begin{bmatrix} 0 & 0 \\ 0 & 0 \\ 1 & 0 \\ 0 & 1 \end{bmatrix}}_{B} \begin{bmatrix} \ddot{x}^{i-1} \\ \ddot{y}^{i-1} \end{bmatrix} + \underbrace{\begin{bmatrix} -\dot{d}_x^i(t) \\ -\dot{d}_y^i(t) \\ 0 \\ 0 \end{bmatrix}}_{\phi(t)} \tag{3.6}$$

or equivalently:

$$\dot{e}^i = Ae^i + Bu^i - Bs^{i-1} + \phi(t) \tag{3.7}$$

where u^i denotes the control input and s^{i-1} is defined as:

$$s^{i-1} := \begin{bmatrix} \ddot{x}^{i-1} \\ \ddot{y}^{i-1} \end{bmatrix}$$

Note that Assumption 3.1 implies $\|\phi(t)\|$ is an exponentially decaying signal, where $\|.\|$ denotes the 2-norm.

Assumption 3.2. *It is assumed that each robot's acceleration is uniformly bounded; i.e.,* $\|s^{i-1}\| \leq \rho$ *for* $i \in \{2,...,n\}$, *where* ρ *is a known constant.*

A control law of the following form is proposed for the followers:

$$u^i = K^i e^i - \frac{B^T P^i e^i}{\|B^T P^i e^i\|}\rho \quad , \quad i \in \{2,...,n\} \tag{3.8}$$

to regulate the position and velocity errors for each follower, where $K^i \in \mathbb{R}^{2\times 4}$ is a constant matrix and $P^i \in \mathbb{R}^{4\times 4}$ is a symmetric positive definite matrix.

Remark 3.1. *In the case when $\|B^T P^i e^i\|$ in (3.8) is "close" to zero, the control input can be modified as follows:*

$$u^i = \begin{cases} K^i e^i - \frac{B^T P^i e^i}{\|B^T P^i e^i\|}\rho & \|B^T P^i e^i\| \geq \vartheta \\ K^i e^i + \vartheta & \|B^T P^i e^i\| < \vartheta \end{cases}, \quad i \in \{2,...,n\}$$

where ϑ is a sufficiently small positive constant.

It is desired to design the control law for the followers such that the steady-state error is as close to zero as possible in the following three scenarios:

- Perfect sensing without input constraint
- Perfect sensing with input constraint
- Noisy measurements

3.3 Main Results

3.3.1 Perfect Sensing without Input Constraint

Theorem 3.1. *Consider a platoon of WMRs moving in formation with leader-follower structure, where the dynamics of the followers obey equation (3.7), and suppose the conditions of Assumptions 3.1 and 3.2 hold. Given $\alpha > 0$, assume also that there exist matrices $R^i > 0$ and S^i satisfying the following LMI:*

$$R^i A^T + AR^i + S^{iT} B^T + BS^i + \alpha R^i < 0 \tag{3.9}$$

If the controller (3.8) with $K^i = S^i R^{i-1}$ and $P^i = R^{i-1}$ is applied to follower i, then $\|e^i(t)\|$ decays exponentially.

Proof: It is straight forward to show that (3.7) under controller (3.8) can be described by:

$$\dot{e}^i = (A+BK^i)e^i - \frac{BB^T P^i e^i}{\|B^T P^i e^i\|}\rho - Bs^{i-1} + \phi(t)$$

Let $V^i = e^{iT} P^i e^i$; then:

$$\begin{aligned}
\dot{V}^i + \xi V^i &= 2e^{iT} P\dot{e}^i + \xi e^{iT} Pe^i \\
&= 2e^{iT} P^i (A+BK^i)e^i - 2\frac{e^{iT} P^i BB^T Pe^i}{\|B^T P^i e^i\|}\rho - 2e^{iT} P^i Bs^{i-1} + 2e^{iT} P^i \phi(t) + \xi e^{iT} P^i e^i \\
&= 2e^{iT} P^i (A+BK^i)e^i - 2\|B^T P^i e^i\|\rho - 2e^{iT} P^i Bs^{i-1} + 2e^{iT} P^i \phi(t) + \xi e^{iT} P^i e^i
\end{aligned} \tag{3.10}$$

where ξ is chosen as:

$$0 < \xi = \min\{\alpha, 2\lambda\} - \varepsilon_0 \tag{3.11}$$

and ε_0 is a sufficiently small positive number. In (3.10), it is required to have

$$-2\|B^T P^i e^i\|\rho - 2e^{iT} P^i Bs^{i-1} < 0$$

or equivalently:

$$|e^{iT} P^i Bs^{i-1}| < \|B^T P^i e^i\|\rho$$

which is known to be valid because:

$$\|A^T\| = \|A\|$$

$$2\|A \times B\| \leq \|A\|^2 \times \|B\|^2$$

On the other hand, using:

$$2AB \leq \|A\|^2 + \|B\|^2$$

the term $2e^{iT}P^i\phi(t)$ can be rewritten as:

$$\begin{aligned}2e^{iT}P^i\phi(t) &= \frac{\sqrt{\sigma}}{\sqrt{\sigma}} \times 2e^{iT}P^i\phi(t) = 2 \times (\sqrt{\sigma}e^{iT}) \times (\frac{1}{\sqrt{\sigma}}P^i\phi(t)) \\ &\leq \|\sqrt{\sigma}e^i\|^2 + \|\frac{1}{\sqrt{\sigma}}P^i\phi(t)\|^2 \\ &\leq \sigma\|e^i\|^2 + \frac{1}{\sigma}\|P^i\phi(t)\|^2\end{aligned}$$

where σ is an arbitrary positive constant. Thus, (3.10) can be modified as:

$$\dot{V}^i + \xi V^i \leq 2e^{iT}P^i(A+BK^i)e^i + \sigma e^{iT}e^i + \frac{1}{\sigma}\|P^i\phi(t)\|^2 + \xi e^{iT}P^i e^i \tag{3.12}$$

By adding and subtracting $\alpha e^{iT}P^i e^i$ from both side of (3.12), one can conclude that:

$$\dot{V}^i + \xi V^i \leq 2e^{iT}P^i(A+BK^i)e^i + \alpha e^{iT}P^i e^i + \frac{1}{\sigma}\|P^i\phi(t)\|^2 - (\alpha-\xi)e^{iT}P^i e^i + \sigma e^{iT}e^i$$

Choose:

$$\sigma < (\alpha-\xi)\lambda_{\min}(P^i) \tag{3.13}$$

so that:

$$-(\alpha-\xi)e^{iT}P^i e^i + \sigma e^{iT}e^i < 0$$

Now, if:

$$(A+BK^i)^T P^i + P^i(A+BK^i) + \alpha P^i < 0 \tag{3.14}$$

then it follows that:

$$\dot{V}^i + \xi V^i - \frac{1}{\sigma}\|P^i\phi(t)\|^2 < 0 \tag{3.15}$$

Multiplying (3.15) by $e^{\xi t}$ yields:

$$\frac{d}{dt}[e^{\xi t}V] < \frac{1}{\sigma}\|P^i\phi(t)\|^2 e^{\xi t}$$

Integrating from t_0 to t, one arrives at:

$$e^{\xi t}V(t) - e^{\xi t_0}V(t_0) < \int_{t_0}^{t} \frac{1}{\sigma}\|P^i\phi(\tau)\|^2 e^{\xi\tau}d\tau$$

or equivalently:

$$V(t) < \frac{1}{\sigma}\int_{t_0}^{t} \|P^i\phi(\tau)\|^2 e^{-\xi(t-\tau)d\tau} + e^{\xi(t_0-t)}V(t_0)$$

Since $\|\phi(t)\|$ is an exponentially decaying signal and $\|\phi(t)\|^2$ has decay rate 2λ, choosing $\xi < 2\lambda$ in (3.11) results in:

$$\lim_{t\to\infty}\int_{t_0}^{t} \|P^i\phi(\tau)\|^2 e^{-\xi(t-\tau)d\tau} \to 0,$$

It is implied from (3.15) that $V^i(t)$ and $e^i(t)$ are also exponentially decaying signals. Now, let $P^i = R^{i^{-1}}$ and $K^i = S^iP^i$; then (3.14) is equivalent to (3.9). ■

Remark 3.2. *It is to be noted that the design parameter α in (3.9) can be chosen properly such that the underlying LMI conditions are feasible. A similar comment can be made on the LMI conditions given in the theorems presented in the sequel.*

3.3.2 Perfect Sensing with Input Constraint

Theorem 3.2. *Consider the system described in Theorem 3.1. Define $\mu_1 = \max||e_{p_x}{}^i|| = \max||e_{p_y}{}^i||$ and $\mu_2 = \max||e_{v_x}{}^i|| = \max||e_{v_y}{}^i||$, and let the design parameters $\alpha > 0$, $\eta > 0$ be given. Solve the following LMIs*

$$R^iA^T + AR^i + S^{i^T}B^T + BS^i + \alpha R^i < 0 \qquad (3.16a)$$

$$\begin{bmatrix} \eta^2 R^i & S^{iT} \\ S^i & I_2 \end{bmatrix} > 0 \tag{3.16b}$$

$$R^i > 4 \begin{bmatrix} {\mu_1}^2 I_2 & 0 \\ 0 & {\mu_2}^2 I_2 \end{bmatrix} \tag{3.16c}$$

where I_2 is the 2×2 identity matrix. If the problem has a feasible solution, then:

i) If the controller (3.8) with $K^i = S^i {R^i}^{-1}$ and $P^i = {R^i}^{-1}$ is applied to follower i, then $\|e^i(t)\|$ is an exponentially decaying signal, and

ii) $||u^i|| < \eta + \rho$.

Proof: The proof is omitted due to its similarity to that of Theorem 2.2. ■

3.3.3 Noisy Measurements

The control law (3.8) in the presence of measurement noise on the follower's motion can be written as:

$$u^i = K^i \tilde{e}^i - \frac{B^T P^i \tilde{e}^i}{\|B^T P^i \tilde{e}^i\|} \rho \tag{3.17}$$

where $\tilde{e}^i = e^i + \delta_e^i$, and δ_e^i is the measurement noise, which is assumed to have a known bound represented by:

$$\Delta_e^i := \max_{t > t_0} ||\delta_e^i||^2$$

In this subsection, an upper bound on the steady-state error is obtained and an algorithm is proposed to design K^i and $P^i > 0$ such that this upper bound is minimized. To this end, the following lemma is presented.

Lemma 3.1. *Assume that $g(t)$ is an exponentially decaying signal. Given $\xi > 0$, let the following inequality hold:*

$$\dot{V} + \xi V - b {\delta_e^i}^T Q \delta_e^i - \|g(t)\|^2 < 0 \tag{3.18}$$

where b is a positive constant and Q is a symmetric positive definite matrix. Then:

$$V(\infty) < \frac{b}{\xi} \max_{t>t_0} [\delta_e^{iT}(t) Q \delta_e^i(t)] \tag{3.19}$$

Proof: Multiplying (3.18) by $e^{\xi t}$ leads to:

$$\frac{d}{dt}[e^{\xi t} V] < b\delta_e^i(t)^T Q \delta_e^i(t) e^{\xi t} + \|g(t)\|^2 e^{\xi t}, \quad \forall t > t_0$$

Integrating both sides from t_0 to t, one arrives at:

$$e^{\xi t} V(t) - e^{\xi t_0} V(t_0) < \int_{t_0}^{t} [b\delta_e^{iT}(\tau) Q \delta_e^i(\tau) + \|g(\tau)\|^2] e^{\xi \tau} d\tau$$

or equivalently:

$$V(t) < \frac{b}{\xi} \max_{t>t_0} [\delta_e^{iT}(t) Q \delta_e^i(t)(e^{\xi t} - e^{\xi t_0})] e^{-\xi t} + e^{\xi(t_0 - t)} V(t_0) + \int_{t_0}^{t} \|g(\tau)\|^2 e^{-\xi(t-\tau)} d\tau$$

Since

$$\lim_{t \to \infty} \int_{t_0}^{t} \|g(\tau)\|^2 e^{-\xi(t-\tau)} d\tau \to 0,$$

hence (3.19) is deduced for $t \to \infty$. ■

Remark 3.3. *Consider the system described in Theorem 3.1. Let $R^i = P^{i-1}$, and assume R^i has a lower bound R_l and an upper bound R_r given in (2.23a) and (2.23b), respectively. Using the result of Theorem 2.3 for each follower, it can be concluded that, if the controller (3.17) with $K^i = S^i R^{i-1}$ and $P^i = R^{i-1}$ is applied to the follower i, then:*

i) $\|e^i(t)\|$ *is an exponentially decaying signal for* $\Delta_e^i = 0$.

ii) $\lim_{t \to \infty} ||e_p^i|| < \bar{e}_{p,\min}$.

An upper bound on the steady-state position error is obtained as (2.33) and Remark 2.2 holds. This is can be proved by choosing $Q = R^{i-1}$, $g(t) = \frac{1}{\sqrt{\sigma}} P^i \phi(t)$, *and* σ *selected as (3.13).*

3.4 Simulation Results

Example 3.1. *Consider two mobile robots, one leader and one follower, and assume the leader moves on a circular track given by:*

$$x_r^l = 2\cos 0.025t$$

$$y_r^l = 2\sin 0.025t$$

The follower is to follow the leader with the following desired distance:

$$d(t) = \begin{bmatrix} d_x(t) \\ d_y(t) \end{bmatrix} = \begin{bmatrix} 1 - 2(1 - e^{-t}) \end{bmatrix} \begin{bmatrix} 1 \\ -1 \end{bmatrix}$$

Similar to Example 2.1, the experiment is to be performed in a 4×4 m *environment; thus,* $\max ||e_{p_x}|| = \max ||e_{p_y}|| = \mu_1 = 4$. *Furthermore, let the maximum speed of the robot be* 0.3 m/sec, *i.e.,* $\max ||e_{v_x}|| = \max ||e_{v_y}|| = \mu_2 = 0.3$. *Consider a control input of the form (3.8), and choose* $\eta = 0.04$. *Now, one can use Theorem 3.2 with* $\alpha = 0.04$ *to obtain the control parameters. In this case, the gain matrix K in (3.8) will be:*

$$K = \begin{bmatrix} -0.0007 & 0 & -0.0420 & 0 \\ 0 & -0.0007 & 0 & -0.0420 \end{bmatrix}$$

In Figure 3.2, the relative position of the follower with respect to the leader along the x-axis is compared with its desired trajectory d_x. *A similar comparison is made in the y direction in Figure 3.3. These figures demonstrate that the desired position tracking is achieved asymptotically. Furthermore, Figure 3.4 shows that the velocity regulation error*

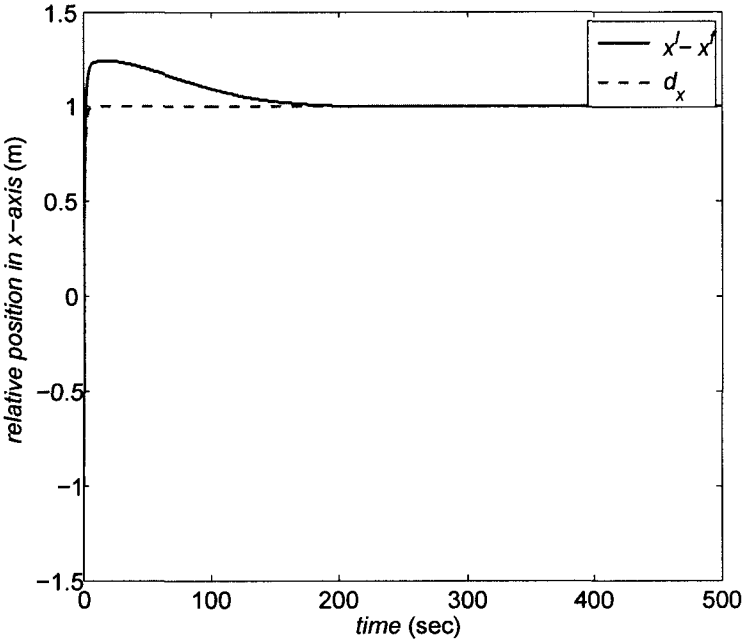

Figure 3.2: Relative position of the follower with respect to the leader along the x-axis for the leader-follower circular trajectory tracking of Example 3.1.

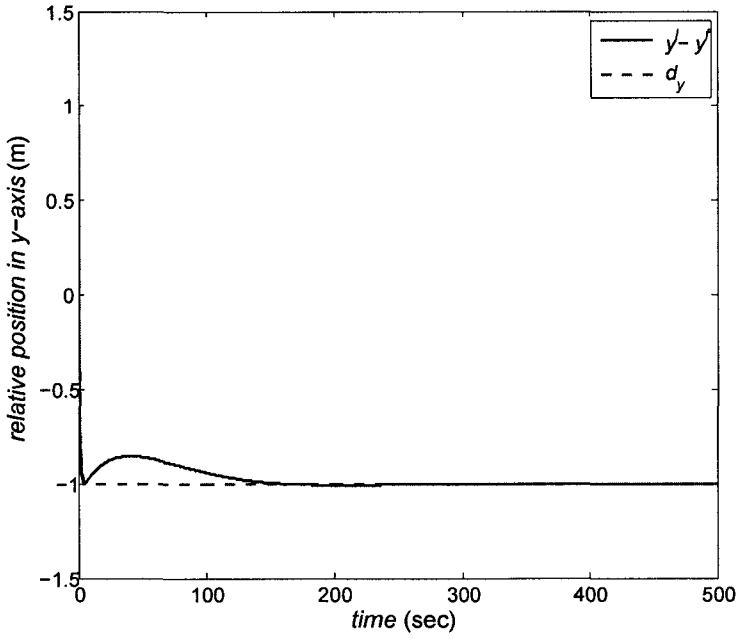

Figure 3.3: Relative position of the follower with respect to the leader along the y-axis for the leader-follower circular trajectory tracking of Example 3.1.

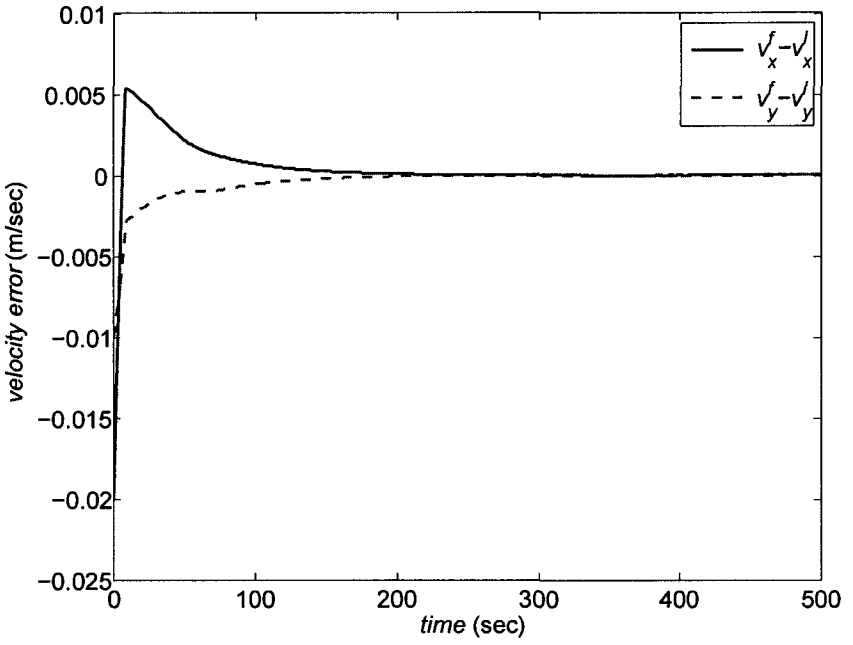

Figure 3.4: The velocity error of the follower for the leader-follower circular trajectory tracking of Example 3.1.

e_v approaches zero in both directions x and y. Figure 3.5 shows the trajectory of the leader and follower moving toward the circular path from their initial positions (1.9,0.1) and (2.8,-0.8), respectively. The norm of the control inputs applied to the follower and leader, $||u^l||$ and $||u^f||$, are depicted in Figure 3.6, which demonstrate that the input constraint is satisfied.

Example 3.2. *Consider a multi-agent system, where 2 followers are to follow a leader in a linear path. Suppose that the leader and followers are initially located on an equilateral triangle with the length of the sides equal to 2* m. *The final desired formation is another equilateral triangle with the length of the sides equal to 1* m, *while the leader is tracking a ramp reference signal along both axes, characterized by:*

$$x_r^l(t) = y_r^l(t) = 0.4t$$

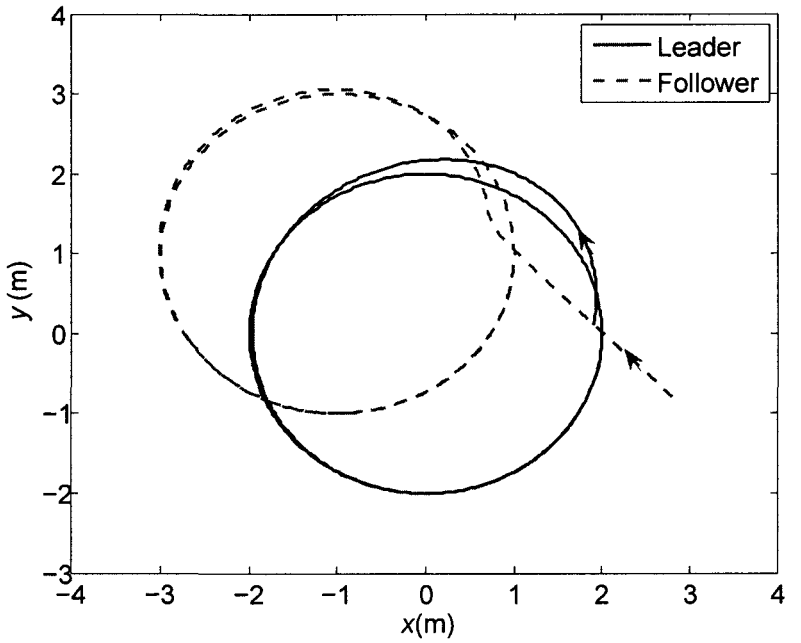

Figure 3.5: The leader and follower trajectories in the 2-D plane for the leader-follower circular trajectory tracking of Example 3.1.

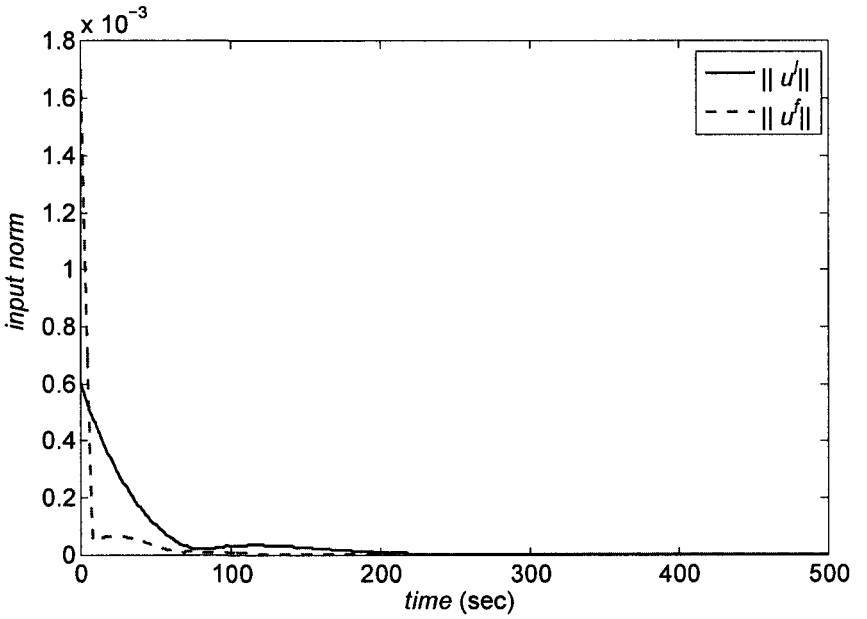

Figure 3.6: Control input norms $||u^f||$ and $||u^l||$ for the leader-follower circular trajectory tracking of Example 3.1.

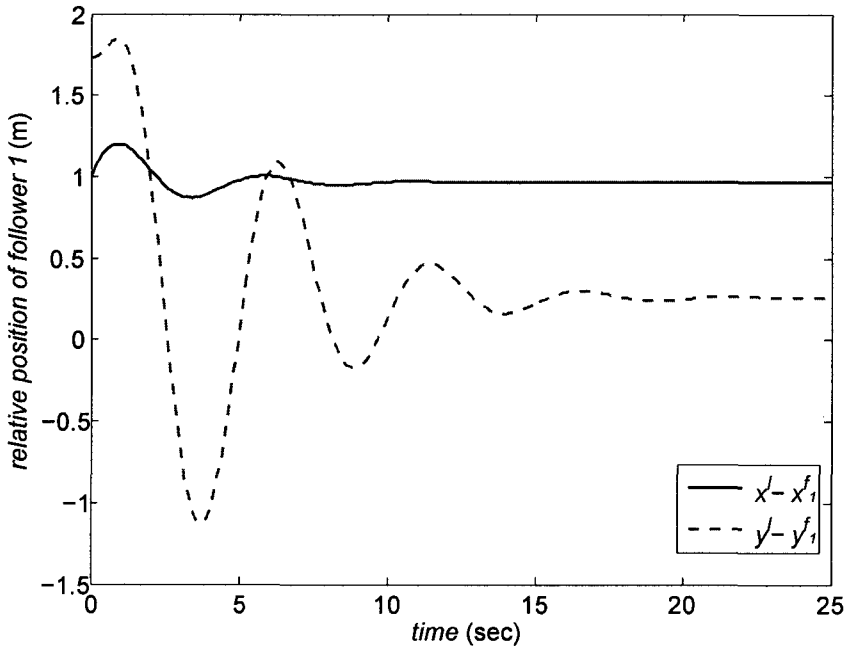

Figure 3.7: Relative position of follower 1 with respect to the leader along the x and y axes for the leader-follower trajectory tracking of Example 3.2.

Let $\alpha = 0.04$, $\Omega_{\beta_1} = -1$, $\Omega_{\beta_2} = -2$, *and* $\Omega_{\gamma_1} = 1$. *Assume that the measurement noise is a random process which is uniformly distributed in the intervals* $(0, 2 \times 10^{-5})$ *and* $(0, 10^{-3})$ *for position and velocity measurements, respectively. Using Remark 3.3 with* $b = 1.55$, *the gain matrix given below is obtained for both followers:*

$$K = \begin{bmatrix} -1.6724 & 0 & -0.7615 & 0 \\ 0 & -1.6724 & 0 & -0.7615 \end{bmatrix}$$

It results from Remark 3.3 that an upper bound for the steady-state position error is 9.7×10^{-3}. *In fact, the steady-state position error obtained from simulation is approximately equal to* 3×10^{-3} *which confirms the theoretical development. Figure 3.7 depicts the relative position of follower 1 with respect to the leader in both directions. The velocity regulation error of follower 1 along the x and y axes is plotted in Figure 3.8. This figure shows that the error approaches zero in both directions. The planar motion of the formation is sketched Figure 3.9.*

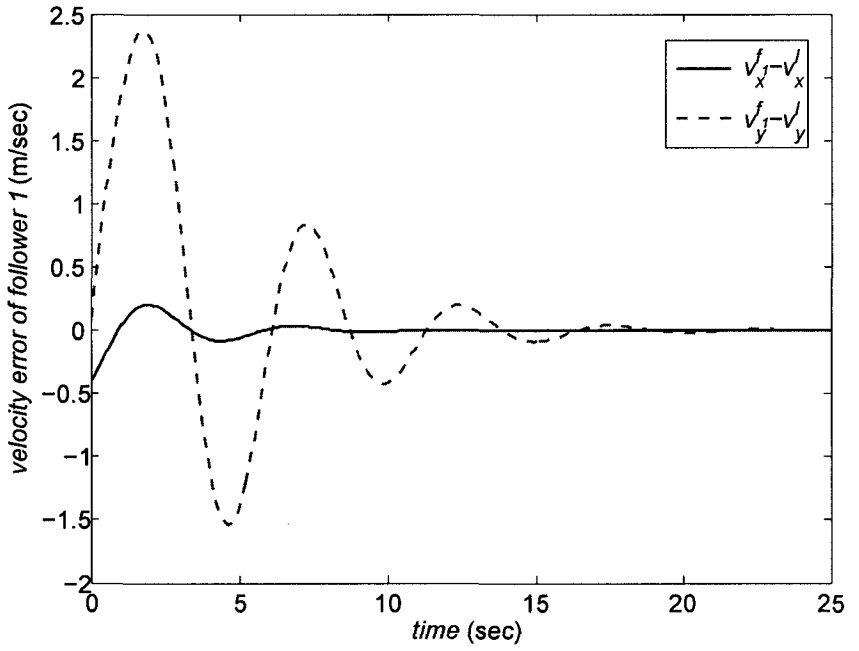

Figure 3.8: The velocity of follower 1 for the leader-follower trajectory tracking of Example 3.2.

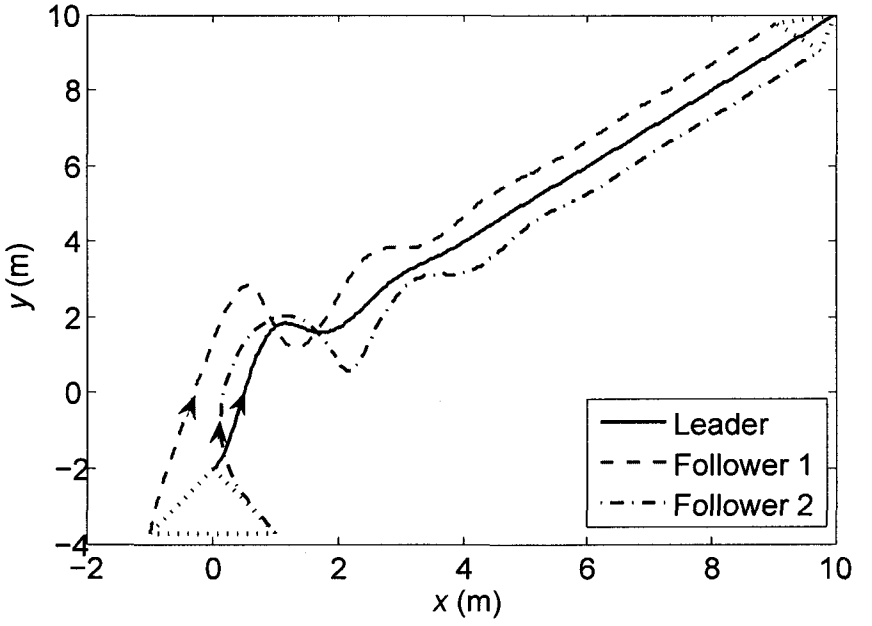

Figure 3.9: The planar motion of the formation for the leader-follower trajectory tracking of Example 3.2.

Chapter 4

Convergence Analysis for a Platoon of Wheeled Mobile Robots Subject to Delay in Control Input and Trajectory Switching

4.1 Introduction

In many real-world applications of the formation control in wheeled mobile robots (WMR), the robots are required to switch between different tracking trajectories. Some examples of this type of strategy include obstacle avoidance in rescue missions, or collision avoidance in autonomous highway systems [59]. While switching in the parameters of the system has been well-investigated in the literature, the problem described above is concerned with switching in the reference input not the system parameters. Nevertheless, some of the important concepts in the stability analysis of switched systems will be borrowed in this chapter to find an error bound in the underlying problem.

On the other hand, a multi-agent system is usually subject to delay in the state,

input or output, due, for example, to communication between agents and control computation. Stability of linear time-delay systems has been extensively studied in the past three decades. In [60], [61] linear matrix inequality (LMI) based approaches are used to find stability conditions for this type of system. LMI-based techniques are also proposed recently for asymptotic and exponential stability of time-delay systems [62]. There are two main approaches to study the stability of time-delay systems: delay-dependent analysis and delay-independent analysis. The stability criteria obtained by using the delay-dependent approach are, in general, less conservative than the ones obtained by the delay-independent approach (note that both methods provide only sufficient conditions for stability).

4.2 Preliminaries

In the analysis of switched systems, it is well-known that if switching between the systems occurs too frequently, the overall system can be unstable even if each individual systems are stable. The notion of *dwell time* was introduced in [63] to provide a sufficient condition for the stability of switched systems in terms of switching speed. In other words, a system which switches between a set of stable systems is stable if the time interval between the consecutive switchings is greater than a certain value, denoted by T_d. Different techniques are provided to find the value of T_d in terms of system parameters (e.g., see [64], [65]).

The stability criterion presented in [63] can be too conservative, in general. The notion of *average dwell time* was then introduced in [66] to remedy this shortcoming of dwell time based stability criterion, by allowing fast switchings provided they will be compensated for by sufficiently slow switchings throughout the process. While these notions are mainly introduced for the stability of systems with parameter jump, they will be used to find an error bound for the tracking problem investigated in this chapter. The

following definition is borrowed from [66].

Definition 4.1. *(Average-dwell time) Denote with $N(T,t)$ the number of discontinuities on the interval (t,T). The average dwell time T_a is defined to be the time between consecutive switches, and is given by:*

$$T_a \geq \frac{T-t}{N_0 - N(T,t)} \quad \forall T \geq t \geq 0. \tag{4.1}$$

where $N_0 > 0$ is called the chatter bound.

In this chapter an obstacle-free environment is used, and is assumed that the desired tracking trajectories of the robots are known *a priori*. The robots are required to follow a trajectory in this known set, in any given time interval, and this trajectory can change instantaneously at the switching instants (which are not necessarily known *a priori*). The convergence properties of the tracking error will then be analyzed by using the Lyapunov technique.

4.3 Main Results

Consider a platoon of mobile robots, and let the set of possible trajectories for robot i be denoted by $\{\phi_1^i, \ldots, \phi_m^i\}$, $\forall i \in \{2, \ldots, r\}$ where r is the number of followers in the platoon. The lemma presented below will prove useful in deriving the main results of this chapter.

Lemma 4.1. *Suppose that the conditions given in Assumptions 3.1 and 3.2 hold. Given the strictly positive real parameters ξ, λ, ε and σ, let the following inequality hold for a Lyapunov function $V(e(t))$:*

$$\dot{V}^i + \xi V^i - \frac{1}{\sigma}\|\phi_j^i(t)\|^2 < \frac{\rho^2}{\varsigma}, \quad \forall i \in \{2, \ldots, r\}, \quad j \in \{1, \ldots, m\} \tag{4.2}$$

where $\phi_j^i(t)$ represents the j-th trajectory which the i-th robot is to follow. Then:

$$V^i(e(t)) \leq e^{-\xi(t-t_0)}V^i(e(t_0)) + (\frac{\varepsilon^2}{\sigma(2\lambda-\xi)})\{e^{-\xi(t-t_0)} - e^{-2\lambda(t-t_0)}\} + \frac{\rho^2}{\varsigma\xi}[1-e^{-\xi(t-t_0)}] \tag{4.3}$$

Proof: From Assumption 3.1, it is known that $\phi_j^i(t)$ is exponentially decaying. Assuming that $\phi_j^i(t)$ has a decay rate λ_j and a gain ε_j, then $\phi^i(t) = \max_{j\in\{1,\ldots,m\}} \phi_j^i(t)$ satisfies the following relation:

$$\phi^i(t) \leq \varepsilon e^{-\lambda(t-t_0)} \tag{4.4}$$

where:

$$\varepsilon = \max_{j\in\{1,\ldots,m\}} \{\varepsilon_j\} \tag{4.5a}$$

$$\lambda = \min_{j\in\{1,\ldots,m\}} \{\lambda_j\} \tag{4.5b}$$

Inequality (4.2) can then be written as:

$$\dot{V}^i + \xi V^i \leq \frac{1}{\sigma}\|\phi^i(t)\|^2 + \frac{\rho^2}{\varsigma} \tag{4.6}$$

Using (4.4), multiplying (4.6) by $e^{\xi t}$, and then integrating both sides from t_0 to t results in:

$$\begin{aligned}
\int_{t_0}^{t} \frac{d}{ds}[e^{\xi s}V^i(e(s))]ds &\leq \frac{1}{\sigma}\int_{t_0}^{t} e^{\xi s}\varepsilon^2 e^{-2\lambda(s-t_0)}ds + \frac{\rho^2}{\varsigma}\int_{t_0}^{t} e^{\xi s}ds \\
e^{\xi t}V^i(e(t)) - e^{\xi t_0}V^i(e(t_0)) &\leq (\frac{1}{\sigma}\varepsilon^2 e^{2\lambda t_0})\int_{t_0}^{t} e^{-(2\lambda-\xi)s}ds + \frac{\rho^2}{\varsigma\xi}[e^{\xi t} - e^{\xi t_0}] \\
&\leq (\frac{-\varepsilon^2 e^{2\lambda t_0}}{\sigma(2\lambda-\xi)})\{e^{-(2\lambda-\xi)t} - e^{-(2\lambda-\xi)t_0}\} + \frac{\rho^2}{\varsigma\xi}[e^{\xi t} - e^{\xi t_0}]
\end{aligned} \tag{4.7}$$

Multiplying both sides of the above relation by $e^{-\xi t}$ yields:

$$V^i(e(t)) \leq e^{-\xi(t-t_0)}V^i(e(t_0)) + (\frac{\varepsilon^2}{\sigma(2\lambda-\xi)})\{e^{-\xi(t-t_0)} - e^{-2\lambda(t-t_0)}\} + \frac{\rho^2}{\varsigma\xi}[1-e^{-\xi(t-t_0)}] \tag{4.8}$$

This completes the proof. ■

4.3.1 Delay in Sensors

In this subsection, the trajectory tracking problem in a platoon of WMRs subject to the measurement delay is formulated in the framework of time-delay systems, and the stability analysis is presented accordingly.

The error dynamics of a platoon of WMRs in a leader-follower structure was obtained in Chapter 3 as:

$$\dot{e}^i(t) = Ae^i(t) + Bu^i(t) - Bs^{i-1}(t) + \phi_j^i(t) \tag{4.9}$$

Now, let the output measurement in the feedback control structure be subject to unknown delay. The resultant closed-loop system can then be modeled as follows:

$$\sum : \begin{cases} \dot{e}^i(t) = Ae^i(t) + Bu^i(t) - Bs^{i-1}(t) + \phi_j^i(t) \\ u^i = K^i e^i(t - \tau(t)) \end{cases} \tag{4.10}$$

where $\tau(t)$ is the time-varying delay which is assumed to be a continuous function of times satisfying the following conditions:

$$\|\tau(t)\| \leq h \tag{4.11a}$$

$$\|\dot{\tau}(t)\| \leq b \tag{4.11b}$$

where $h > 0$ and $0 < b < 1$ are known values. The following theorem provides conditions under which the time-delay system (4.10) is exponentially stable.

Theorem 4.1. *Consider closed-loop system (4.10), and assume the time-delay satisfies the conditions in (4.11). Let the conditions of Assumptions 3.1 and 3.2 hold. Assume also*

that for any given constants $\alpha > 0$, $0 < \xi < \alpha$, *the gain matrix* K^i, *there exist symmetric matrices* $P^i > 0$, $Q^i \geq 0$, $Z^i \geq 0$, $i = 1,2$, *constants* $\delta_1 > 0$, $\delta_2 > 0$, $\varsigma_1 > 0$, *and a matrix* $N = [N_1 \;\; N_2]^T$ *such that the following LMI holds:*

$$\Xi = \begin{bmatrix} \mathscr{E} + h\begin{bmatrix} Z_1^i & 0 \\ 0 & Z_2^i \end{bmatrix} + \begin{bmatrix} N_1 + N_1^T & -N_1 + N_2^T \\ -N_1^T + N_2 & -N_2 - N_2^T \end{bmatrix} & hN\begin{bmatrix} A & BK^i \end{bmatrix} & hNB & hN & \begin{bmatrix} P^iB \\ 0 \end{bmatrix} \\ * & -h\begin{bmatrix} Z_1^i & 0 \\ 0 & Z_2^i \end{bmatrix} e^{-\xi h} & 0 & 0 & 0 \\ * & * & -h\delta_1 & 0 & 0 \\ * & * & * & -h\delta_2 & 0 \\ * & * & * & * & -\varsigma_1 \end{bmatrix} < 0 \tag{4.12}$$

where

$$\mathscr{E} = \begin{bmatrix} P^iA + A^TP^i + Q^i + \alpha P^i & P^iBK^i \\ K^{iT}B^TP^i & -(1-b)Q^ie^{-\xi h} \end{bmatrix} \tag{4.13}$$

and $*$ *denotes the symmetric terms in a symmetric matrix. Then, under the controller (4.10) the solution of the system (4.9) is exponentially convergent to the ball* $\mathscr{B}(r)$ *with the rate* $\bar{\lambda} = \frac{1}{2}\xi$, *where r is defined as follows:*

$$r = \sqrt{\frac{\rho^2}{\xi\varsigma\lambda_{min}(P^i)}} \tag{4.14}$$

and

$$\varsigma = \frac{1}{\varsigma_1 + h\delta_1}$$

Proof: Define the positive-defintie Lyapunov-Krasovskii functional as follows:

$$V^i = e^{iT}P^i e^i + \int_{t-\tau(t)}^{t} e^{iT}(q)Q^i e^{\xi(q-t)}e^i(q)dq + \int_{-h}^{0}\int_{t+\theta}^{t}\begin{bmatrix} e^i(q) \\ e^i(q-\tau(q)) \end{bmatrix}^T \begin{bmatrix} Z_1^i & 0 \\ 0 & Z_2^i \end{bmatrix} e^{\xi(q-t)} \begin{bmatrix} e^i(q) \\ e^i(q-\tau(q)) \end{bmatrix} dqd\theta \tag{4.15}$$

where P^i is a symmetric positive-definite matrix, and Q^i, Z_1^i, Z_2^i are symmetric positive semi-definite matrices.

The derivative of the Lyapunov-Krasovskii functional (4.15) along the trajectories of system (4.10) with the given controller, is obtained as:

$$\begin{aligned}\dot{V}^i + \xi V^i \leq & e^{iT}(P^iA + A^TP^i)e^i + 2e^{iT}P^iBK^ie^i(t-\tau(t)) + e^{iT}Q^ie^i \\ & -(1-b)e^{iT}(t-\tau(t))Q^ie^{-\xi h}e^i(t-\tau(t)) + \xi e^{iT}P^ie^i - 2e^{iT}P^iBs^{i-1} + 2e^{iT}P^i\phi^i(t) \\ & + h\begin{bmatrix} e^i(t) \\ e^i(t-\tau(t)) \end{bmatrix}^T \begin{bmatrix} Z_1^i & 0 \\ 0 & Z_2^i \end{bmatrix} \begin{bmatrix} e^i(t) \\ e^i(t-\tau(t)) \end{bmatrix} \\ & - \int_{t-\tau(t)}^{t} \begin{bmatrix} e^i(q) \\ e^i(q-\tau(q)) \end{bmatrix}^T \begin{bmatrix} Z_1^i & 0 \\ 0 & Z_2^i \end{bmatrix} e^{-\xi h} \begin{bmatrix} e^i(q) \\ e^i(q-\tau(q)) \end{bmatrix} dq \end{aligned} \tag{4.16}$$

Note that always exist strictly positive constants ς_1, σ_1 such that

$$-2e^{iT}P^iBs^{i-1} \leq \frac{\|e^{iT}P^iB\|^2}{\varsigma_1} + \rho^2\varsigma_1$$

$$2e^{iT}P^i\phi^i(t) \leq \sigma_1\|e^i\|^2 + \frac{1}{\sigma_1}\|P^i\phi^i(t)\|^2$$

Thus, (4.16) can be rewritten as follows:

$$\begin{aligned}\dot{V}^i+\xi V^i \leq\ & e^{iT}(P^iA+A^TP^i)e^i+2e^{iT}P^iBK^ie^i(t-\tau(t))+\sigma_1 e^{iT}e^i+e^{iT}Q^ie^i+\xi e^{iT}P^ie^i\\ & -(1-b)e^{iT}(t-\tau(t))Q^ie^{-\xi h}e^i(t-\tau(t))+\frac{\|e^{iT}P^iB\|^2}{\varsigma_1}+\rho^2\varsigma_1+\frac{1}{\sigma_1}\|P^i\phi^i(t)\|^2\\ & +h\begin{bmatrix}e^i(t)\\ e^i(t-\tau(t))\end{bmatrix}^T\begin{bmatrix}Z_1^i & 0\\ 0 & Z_2^i\end{bmatrix}\begin{bmatrix}e^i(t)\\ e^i(t-\tau(t))\end{bmatrix}\\ & -\int_{t-\tau(t)}^{t}\begin{bmatrix}e^i(q)\\ e^i(q-\tau(q))\end{bmatrix}^T\begin{bmatrix}Z_1^i & 0\\ 0 & Z_2^i\end{bmatrix}e^{-\xi h}\begin{bmatrix}e^i(q)\\ e^i(q-\tau(q))\end{bmatrix}dq\end{aligned} \tag{4.17}$$

Now, by adding and subtracting $\alpha e^{iT}P^ie^i$ one can conclude that:

$$\begin{aligned}\dot{V}^i+\xi V^i \leq\ & e^{iT}(P^iA+A^TP^i)e^i+2e^{iT}P^iBK^ie^i(t-\tau(t))+\alpha e^{iT}P^ie^i+e^{iT}Q^ie^i\\ & -(\alpha-\xi)e^{iT}P^ie^i+\sigma_1 e^{iT}e^i+\frac{e^{iT}P^iBB^TP^ie^i}{\varsigma_1}\\ & -(1-b)e^{iT}(t-\tau(t))Q^ie^{-\xi h}e^i(t-\tau(t))+\rho^2\varsigma_1+\frac{1}{\sigma_1}\|P^i\phi^i(t)\|^2\\ & +h\begin{bmatrix}e^i(t)\\ e^i(t-\tau(t))\end{bmatrix}^T\begin{bmatrix}Z_1^i & 0\\ 0 & Z_2^i\end{bmatrix}\begin{bmatrix}e^i(t)\\ e^i(t-\tau(t))\end{bmatrix}\\ & -\int_{t-\tau(t)}^{t}\begin{bmatrix}e^i(q)\\ e^i(q-\tau(q))\end{bmatrix}^T\begin{bmatrix}Z_1^i & 0\\ 0 & Z_2^i\end{bmatrix}e^{-\xi h}\begin{bmatrix}e^i(q)\\ e^i(q-\tau(q))\end{bmatrix}dq\end{aligned} \tag{4.18}$$

Choose $\sigma_1 < (\alpha-\xi)\lambda_{\min}(P^i)$ and substitute (4.13) in (4.18) to obtain:

$$\dot{V}^i + \xi V^i \leq \begin{bmatrix} e^i(t) \\ e^i(t-\tau(t)) \end{bmatrix}^T \left(\mathscr{E} + h \begin{bmatrix} Z_1^i & 0 \\ 0 & Z_2^i \end{bmatrix} + \begin{bmatrix} \frac{P^i B B^T P^i}{\varsigma_1} & 0 \\ 0 & 0 \end{bmatrix} \right) \begin{bmatrix} e^i(t) \\ e^i(t-\tau(t)) \end{bmatrix}$$
$$- \int_{t-\tau(t)}^{t} \begin{bmatrix} e^i(q) \\ e^i(q-\tau(q)) \end{bmatrix}^T \begin{bmatrix} Z_1^i & 0 \\ 0 & Z_2^i \end{bmatrix} e^{-\xi h} \begin{bmatrix} e^i(q) \\ e^i(q-\tau(q)) \end{bmatrix} dq$$
$$+ \rho^2 \varsigma_1 + \frac{1}{\sigma_1} \|P^i \phi^i(t)\|^2 \tag{4.19}$$

According to the Leibnitz-Newton formula:

$$e(t) - e(t-\tau(t)) - \int_{t-\tau(t)}^{t} \dot{e}(q)dq = 0 \tag{4.20}$$

Using (4.20) and considering an appropriately dimensioned matrix $N = \begin{bmatrix} N_1 & N_2 \end{bmatrix}^T$ one arrives at:

$$2 \begin{bmatrix} e^i(t) \\ e^i(t-\tau(t)) \end{bmatrix}^T N \left[e(t) - e(t-\tau(t)) - \int_{t-\tau(t)}^{t} \dot{e}(q)dq \right] = 0 \tag{4.21}$$

Substituting $\dot{e}$ from (4.10) in (4.21) one can obtain:

$$2 \begin{bmatrix} e^i(t) \\ e^i(t-\tau(t)) \end{bmatrix}^T N \left[e(t) - e(t-\tau(t)) - \int_{t-\tau(t)}^{t} \left(Ae^i(q) + BK^i e^i(q-\tau(q)) - Bs^{i-1}(q) + \phi^i(q) \right) dq \right] = 0 \tag{4.22}$$

Adding (4.22) to the right-hand side of (4.19) yields:

$$\begin{aligned}
\dot{V}^i + \xi V^i \leq & \begin{bmatrix} e^i(t) \\ e^i(t-\tau(t)) \end{bmatrix}^T \left(\mathscr{E} + h \begin{bmatrix} Z_1^i & 0 \\ 0 & Z_2^i \end{bmatrix} + \begin{bmatrix} \frac{P^i B B^T P^i}{\varsigma_1} & 0 \\ 0 & 0 \end{bmatrix} + \begin{bmatrix} N_1 + N_1^T & -N_1 + N_2^T \\ -N_1^T + N_2 & -N_2 - N_2^T \end{bmatrix} \right) \begin{bmatrix} e^i(t) \\ e^i(t-\tau(t)) \end{bmatrix} \\
& - \int_{t-\tau(t)}^{t} \left(\begin{bmatrix} e^i(q) \\ e^i(q-\tau(q)) \end{bmatrix}^T \begin{bmatrix} Z_1^i & 0 \\ 0 & Z_2^i \end{bmatrix} e^{-\xi h} + \begin{bmatrix} e^i(t) \\ e^i(t-\tau(t)) \end{bmatrix}^T N \begin{bmatrix} A & BK^i \end{bmatrix} \right) \begin{bmatrix} Z_1^i & 0 \\ 0 & Z_2^i \end{bmatrix}^{-1} e^{\xi h} \\
& \qquad \left(\begin{bmatrix} Z_1^i & 0 \\ 0 & Z_2^i \end{bmatrix} e^{-\xi h} \begin{bmatrix} e^i(q) \\ e^i(q-\tau(q)) \end{bmatrix} + \begin{bmatrix} A & BK^i \end{bmatrix}^T N^T \begin{bmatrix} e^i(t) \\ e^i(t-\tau(t)) \end{bmatrix} \right) dq \\
& + h \begin{bmatrix} e^i(t) \\ e^i(t-\tau(t)) \end{bmatrix}^T N \begin{bmatrix} A & BK^i \end{bmatrix} \begin{bmatrix} Z_1^i & 0 \\ 0 & Z_2^i \end{bmatrix}^{-1} e^{\xi h} \begin{bmatrix} A & BK^i \end{bmatrix}^T N^T \begin{bmatrix} e^i(t) \\ e^i(t-\tau(t)) \end{bmatrix} \\
& + h \begin{bmatrix} e^i(t) \\ e^i(t-\tau(t)) \end{bmatrix}^T N B \delta_1^{-1} B^T N^T \begin{bmatrix} e^i(t) \\ e^i(t-\tau(t)) \end{bmatrix} + h\rho^2 \delta_1 \\
& + h \begin{bmatrix} e^i(t) \\ e^i(t-\tau(t)) \end{bmatrix}^T N \delta_2^{-1} N^T \begin{bmatrix} e^i(t) \\ e^i(t-\tau(t)) \end{bmatrix} + h \|\phi^i(t)\|^2 \delta_2 \\
& + \rho^2 \varsigma_1 + \frac{1}{\sigma_1} \|P^i \phi^i(t)\|^2
\end{aligned} \tag{4.23}$$

Suppose that there exist strictly positive constants σ and ς such that:

$$\frac{1}{\sigma_1} \|P^i \phi^i(t)\|^2 + h \|\phi^i(t)\|^2 \delta_2 \leq \frac{1}{\sigma} \|\phi^i(t)\|^2$$

$$\rho^2 \varsigma_1 + h\rho^2 \delta_1 \leq \frac{\rho^2}{\varsigma}$$

which yields:

$$\sigma \geq \frac{\sigma_1}{\lambda_{min}(P^i) + h\delta_2 \sigma_1} \tag{4.24a}$$

$$\varsigma \geq \frac{1}{\varsigma_1 + h\delta_1} \tag{4.24b}$$

From the Schur complement, (4.23) can be written as:

$$\dot{V}^i + \xi V^i \leq \Xi + \frac{1}{\sigma}||\phi^i(t)||^2 + \frac{\rho^2}{\varsigma} \tag{4.25}$$

Therefore, if (4.12) holds, it can be concluded that:

$$\dot{V}^i + \xi V^i - \frac{1}{\sigma}\|\phi^i(t)\|^2 < \frac{\rho^2}{\varsigma} \tag{4.26}$$

Now, using Lemma 4.1 and on noting that $\lambda_{\min}(P^i)||e(t)||^2 \leq V^i$, one arrives at:

$$||e(t)|| \leq e^{-\bar{\lambda}(t-t_0)}\psi + \sqrt{\frac{\rho^2}{\xi\varsigma\lambda_{min}(P^i)}} \tag{4.27}$$

where ψ is a positive constant and $\bar{\lambda} = \frac{1}{2}\xi$. This completes the proof. ■

Remark 4.1. *The control gain K^i here is chosen in such a way that it stabilizes the system without delay, i.e., the eigenvalues of $A + BK^i$ are located in the open left-half.*

4.3.2 Switching Trajectories

It is desired in the sequel to find the *dwell time* between the consecutive switchings for each robot in the presence of delay in control input, such that the system remains exponentially convergent to a ball with a specific radius.

For simplicity, the Lyapunov function $V^i(e(t))$ found in Lemma 4.1 will hereafter be represented in the following from:

$$V^i(e(t)) \leq e^{-\xi(t-t_0)}V^i(e(t_0)) + \gamma\{e^{-\xi(t-t_0)} - e^{-2\lambda(t-t_0)}\} + \frac{\rho^2}{\varsigma\xi}[1 - e^{-\xi(t-t_0)}]$$

where:

$$\gamma = \frac{\varepsilon^2}{\sigma(2\lambda - \xi)} \tag{4.28}$$

Since the robots switch between different formations, the desired relative position between any pair of neighboring robots i and $i-1$ ($i \in \{2,\ldots,r\}$) defined by $(d_x^i(t), d_y^i(t))$, might follow different set points in different time intervals. It is desired now to find out how fast these trajectories can switch such that system (4.10) is guaranteed to remains stable. It is assumed that the trajectories $(d_x^i(t), d_y^i(t))$, $i \in \{2,\ldots,r\}$, are continuous at switching times. The extension of the results obtained here to the case where the trajectories are not continuous at the switching instants straightforward. The following two theorems show that system (4.10) is exponentially convergent to a specific ball under the dwell time or average dwell time conditions.

4.3.2.1 Dwell Time

Theorem 4.2. *Suppose that the conditions of Assumptions 3.1 and 3.2 are satisfied with the parameters given in (4.4). Denote with T_{d_i} the dwell time between two consecutive switchings of the relative position of robot i with respect to robot $i-1$. Then, the error signal $e(t)$ in (4.10) exponentially converges to the ball $\mathscr{B}(r)$, where the radius r is given by:*

$$r = \sqrt{(\gamma\{(\frac{\xi}{2\lambda})^{\frac{\xi}{2\lambda-\xi}} - (\frac{\xi}{2\lambda})^{\frac{2\lambda}{2\lambda-\xi}}\} + \frac{\rho^2}{\varsigma\xi})\{\frac{1}{\lambda_{\min}(P^i)(1-e^{-\xi T_{d_i}})}\}} \tag{4.29}$$

The constants σ and ς in the above equation are chosen such that the relations (4.24) are satisfied for $\sigma_1 < (\alpha-\xi)\lambda_{min}(P^i)$, where $\alpha > 0$, $0 < \xi < \alpha$. Furthermore, the matrix P^i and scalars ς_1, δ_1 and δ_2 are found by solving the LMI (4.12) in Theorem 4.1.

Proof: Denote the switching instants with $\{t_k\}$, $k \in \mathbf{Z}$. From (4.3), the quantities $V^i(e(t_1)), V^i(e(t_2)), \ldots, V^i(e(t_N))$ satisfy the relations given below:

$$V^i(e(t_1)) \leq e^{-\xi(t_1-t_0)}V^i(e(t_0)) + \gamma\{e^{-\xi(t_1-t_0)} - e^{-2\lambda(t_1-t_0)}\} + \frac{\rho^2}{\varsigma\xi}[1-e^{-\xi(t_1-t_0)}],$$

$$\forall t \in [t_0, t_1) \tag{4.30a}$$

$$
\begin{aligned}
V^i(e(t_2)) &\le e^{-\xi(t_2-t_1)}V^i(e(t_1)) + \gamma\{e^{-\xi(t_2-t_1)} - e^{-2\lambda(t_2-t_1)}\} + \frac{\rho^2}{\varsigma\xi}[1-e^{-\xi(t_2-t_1)}] \\
&\le e^{-\xi(t_2-t_0)}V^i(e(t_0)) \\
&+ e^{-\xi(t_2-t_1)}\gamma\{e^{-\xi(t_1-t_0)} - e^{-2\lambda(t_1-t_0)}\} + \gamma\{e^{-\xi(t_2-t_1)} - e^{-2\lambda(t_2-t_1)}\} \\
&+ e^{-\xi(t_2-t_1)}\frac{\rho^2}{\varsigma\xi}[1-e^{-\xi(t_1-t_0)}] + \frac{\rho^2}{\varsigma\xi}[1-e^{-\xi(t_2-t_1)}] \\
&\le e^{-\xi(t_2-t_0)}V^i(e(t_0)) + \gamma\sum_{k=1}^{2}\{e^{-\xi(t_2-t_k)}(e^{-\xi(t_k-t_{k-1})} - e^{-2\lambda(t_k-t_{k-1})})\} \\
&+ \frac{\rho^2}{\varsigma\xi}\sum_{k=1}^{2}e^{-\xi(t_2-t_k)}(1-e^{-\xi(t_k-t_{k-1})}), \quad \forall t \in [t_1, t_2)
\end{aligned}
\tag{4.30b}
$$

$$\vdots$$

$$
\begin{aligned}
V^i(e(t_N)) &\le e^{-\xi(t_N-t_0)}V^i(e(t_0)) + \gamma\sum_{k=1}^{N}\{e^{-\xi(t_N-t_k)}(e^{-\xi(t_k-t_{k-1})} - e^{-2\lambda(t_k-t_{k-1})})\} \\
&+ \frac{\rho^2}{\varsigma\xi}\sum_{k=1}^{N}e^{-\xi(t_N-t_k)}(1-e^{-\xi(t_k-t_{k-1})}), \quad \forall t \in [t_{N-1}, t_N)
\end{aligned}
\tag{4.30c}
$$

Note that:

$$Max\{e^{-\xi(t_k-t_{k-1})} - e^{-2\lambda(t_k-t_{k-1})}\} = e^{-\xi t_s^*} - e^{-2\lambda t_s^*}$$

where:

$$t_s^* = \frac{ln(\frac{\xi}{2\lambda})}{\xi - 2\lambda}$$

On the other hand, since:

$$\sum_{k=1}^{N}e^{-\xi(t_N-t_k)}(1-e^{-\xi(t_k-t_{k-1})}) \le \sum_{k=1}^{N}e^{-\xi(t_N-t_k)}$$

therefore, (4.30c) can be rewritten as:

$$V^i(e(t_N)) \le e^{-\xi(t_N-t_0)}V^i(e(t_0)) + \gamma\{e^{-\xi t_s^*} - e^{-2\lambda t_s^*}\}\sum_{k=1}^{N}e^{-\xi(t_N-t_k)} + \frac{\rho^2}{\varsigma\xi}\sum_{k=1}^{N}e^{-\xi(t_N-t_k)} \tag{4.31}$$

Define now:

$$\zeta_f = \gamma\{(\frac{\xi}{2\lambda})^{\frac{\xi}{2\lambda-\xi}} - (\frac{\xi}{2\lambda})^{\frac{2\lambda}{2\lambda-\xi}}\}$$

and let:

$$t_k - t_{k-1} \geq T_{d_i}$$

Hence, (4.31) reduces to:

$$V^i(e(t_N)) \leq e^{-N\xi T_{d_i}} V^i(e(t_0)) + (\zeta_f + \frac{\rho^2}{\varsigma\xi}) \sum_{k=1}^{N} e^{-\xi(t_N - t_k)} \tag{4.32}$$

or equivalently:

$$V^i(e(t_N)) \leq e^{-N\xi T_{d_i}} V^i(e(t_0)) + (\zeta_f + \frac{\rho^2}{\varsigma\xi}) \times \frac{1}{1 - e^{-\xi T_{d_i}}} \tag{4.33}$$

which means that the system error converges to the ball $\mathscr{B}(r)$, with r given by (4.29). ■

4.3.2.2 Average Dwell Time

As discussed earlier in this chapter, the dwell time condition can be too restrictive in practice. Thus, as a more relaxed alternative to the dwell time condition, in this subsection the average dwell time condition will be derived for the trajectory switching

In the following theorem, the radius of the ball to which the tracking error exponentially converges, will be obtained in terms of the average dwell time.

Theorem 4.3. *Assume that the reference trajectory (v_x, v_y) of the i-th robot in t_k, $k \in \mathbf{Z}$, and that the conditions in Assumptions 3.1 and 3.2 hold with the parameters given in (4.4). Denote with T_{a_i} the average dwell time for N consecutive switchings of the relative position of robot i with respect to robot $i-1$. Then, the error signal $e(t)$ in (4.10) exponentially converges to the ball $\mathscr{B}(r)$, where the radius r is given by:*

$$r = \sqrt{(\gamma\{(\frac{\xi}{2\lambda})^{\frac{\xi}{2\lambda-\xi}} - (\frac{\xi}{2\lambda})^{\frac{2\lambda}{2\lambda-\xi}}\} + \frac{\rho^2}{\varsigma\xi})\{\frac{1}{1 - e^{-\xi T_{a_i}}} + N_0\} \times \{\frac{1}{\lambda_{\min}(P^i)}\}} \tag{4.34}$$

The constants σ and ς in the above equation are chosen such that the relations (4.24) are

satisfied for $\sigma_1 < (\alpha - \xi)\lambda_{min}(P^i)$, *where* $\alpha > 0$, $0 < \xi < \alpha$. *Furtheremore, the matrix* P^i *and scalars* ς_1, δ_1 *and* δ_2 *are found by solving the LMI (4.12) in Theorem 4.1, and* N_0 *is a positive constant given in the definition of average dwell time(4.1).*

Proof: The following upper bound we obtained in Theorem 4.2 for a system with N consecutive trajectory switchings:

$$V^i(e(t_N)) \leq e^{-\xi(t_N - t_0)} V^i(e(t_0)) + (\zeta_f + \frac{\rho^2}{\varsigma\xi}) \sum_{k=1}^{N} e^{-\xi(t_N - t_k)} \tag{4.35}$$

For any $N > N_0 + 1$, the above relation can be rewritten as:

$$V^i(e(t_N)) \leq e^{-\xi(t_N - t_0)} V^i(e(t_0)) + (\zeta_f + \frac{\rho^2}{\varsigma\xi})\{ \sum_{k=1}^{N-N_0-1} e^{-\xi(t_N - t_k)} + \sum_{k=N-N_0}^{N} e^{-\xi(t_N - t_k)}\} \tag{4.36}$$

Let $k < N - N_0$; by definition:

$$N(t_N, t_k) - N_0 \leq \frac{t_N - t_k}{T_{a_i}}$$

Since $N(t_N, t_k) = N - k$, this implies that,

$$T_{a_i}(N - N_0 - k) \leq t_N - t_k \tag{4.37}$$

Using (4.37), the relation (4.36) can be expressed as:

$$V^i(e(t_N)) \leq e^{-\xi(N-N_0)T_{a_i}} V^i(e(t_0)) + (\zeta_f + \frac{\rho^2}{\varsigma\xi})\{\frac{e^{-\xi T_{a_i}} - e^{-(N-N_0)\xi T_{a_i}}}{1 - e^{-\xi T_{a_i}}} + 1 + N_0\}$$

Now, as $N \to \infty$:

$$V^i(e(\infty)) \leq (\zeta_f + \frac{\rho^2}{\varsigma\xi})\{\frac{1}{1 - e^{-\xi T_{a_i}}} + N_0\} \tag{4.38}$$

This means that the error $e(t)$ exponentially converges to the ball $\mathscr{B}(r)$, where r is given by (4.34). ■

4.4 Simulation Results

In this section, some simulations are presented to demonstrate the efficiency of the results obtained. In the first example, a trajectory tracking system with time varying delay is studies. Example 2 presents a time-delay leader-follower system with switching between tracking trajectories.

Example 4.1. *Consider a leader-follower system consisting of two agents subject to time delay in the error measurement. Assume that the error dynamics and control input are governed by (4.10), where :*

$$A = \begin{bmatrix} 0 & 0 & 1 & 0 \\ 0 & 0 & 0 & 1 \\ 0 & 0 & 0 & 0 \\ 0 & 0 & 0 & 0 \end{bmatrix}, \quad B = \begin{bmatrix} 0 & 0 \\ 0 & 0 \\ 1 & 0 \\ 0 & 1 \end{bmatrix} \tag{4.39a}$$

$$\tau(t) = 0.15 + 0.1\sin 2t$$

$$K = \begin{bmatrix} -4.0000 & 0 & -3.0000 & 0 \\ 0 & -4.0000 & 0 & -3.0000 \end{bmatrix} \tag{4.39b}$$

Assume also that the leader is supposed to track a circular path given by:

$$x_r^l = 2\cos 0.025t$$

$$y_r^l = 2\sin 0.025t$$

The follower, on the other hand, is to follow the leader with the following desired distance:

$$d(t) = \begin{bmatrix} d_x(t) \\ d_y(t) \end{bmatrix} = \begin{bmatrix} 1 - 2(1 - e^{-t}) \end{bmatrix} \begin{bmatrix} 1 \\ -1 \end{bmatrix}$$

It is straightforward to find the bounds in (4.11) as $h = 0.25$ and $b = 0.2$. Now, using

Theorem 4.1, and solving (4.12) with the parameters $\alpha = 0.2$ *and* $\xi = 0.1$ *one arrives at:*

$$P = \begin{bmatrix} 227.3297 & 0 & 71.2285 & 0 \\ 0 & 227.3297 & 0 & 71.2285 \\ 71.2285 & 0 & 78.0058 & 0 \\ 0 & 71.2285 & 0 & 78.0058 \end{bmatrix} \tag{4.40}$$

$$\varsigma_1 = 1.7269 \times 10^3, \quad \delta_1 = 3.4201 \times 10^3, \quad \rho = 0.0013$$

Now, it results from Theorem 4.1 that $\bar{\lambda} = 0.05$ *and* $r = 0.0286$*, and hence:*

$$||e(t)|| \leq e^{-0.05(t-t_0)}\psi + 0.0286.$$

In Figure 4.1, the relative position of the follower with respect to the leader along the x-axis is compared with its desired trajectory d_x*. A similar comparison is made in the y direction in Figure 4.2.*

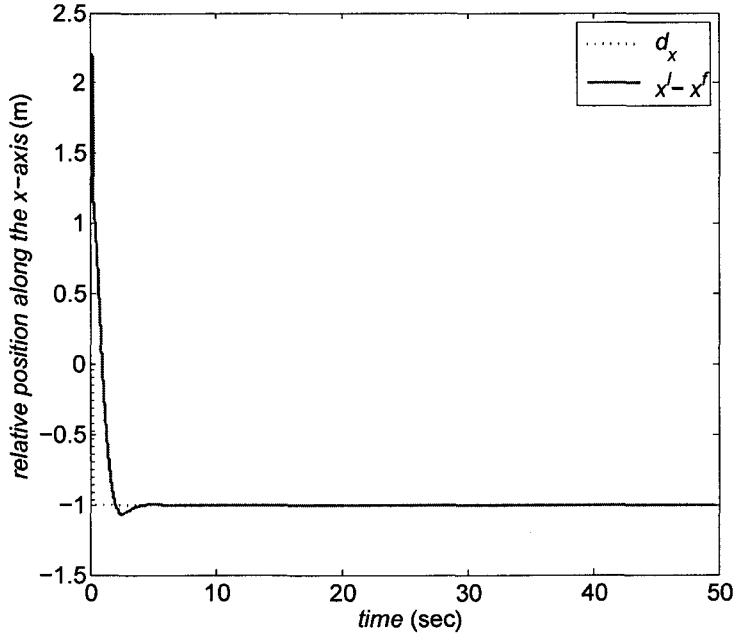

Figure 4.1: The relative position of the follower with respect to the leader along the x-axis for the leader-follower circular trajectory tracking of Example 4.1.

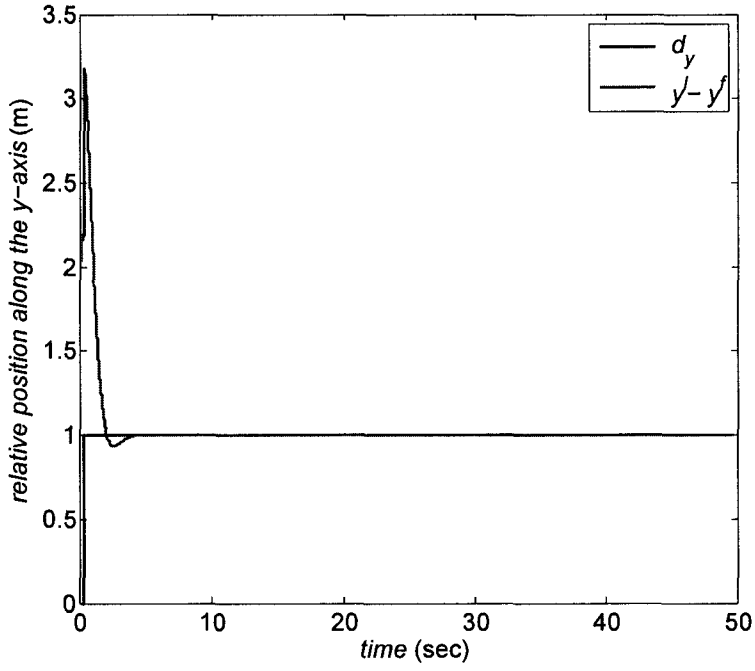

Figure 4.2: The relative position of the follower with respect to the leader along the y-axis for the leader-follower circular trajectory tracking of Example 4.1.

Figure 4.3 depicts the trajectory of the leader together with the follower, and demonstrates that the agents track their desired path asymptotically. Furthermore, simulations were carried out and it was observed that the closed-loop system becomes unstable for $\|\tau(t)\| > 0.3$ *(note that a delay of this size violates the sufficient conditions for stability).*

Example 4.2. *In this example, it is assumed that the desired trajectory of the follower switches between three different functions in equidistance time intervals as drawn in Figure 4.4 and Figure 4.5.*

Assume $\tau(t) = 0.15 + 0.1sin2t$*; in this case,* $h = 0.25$ *and* $b = 0.2$*. Now, using Theorem 4.1 with* $\alpha = 0.2$ *and* $\xi = 0.1$ *and the same control gain as (4.39b) yields:*

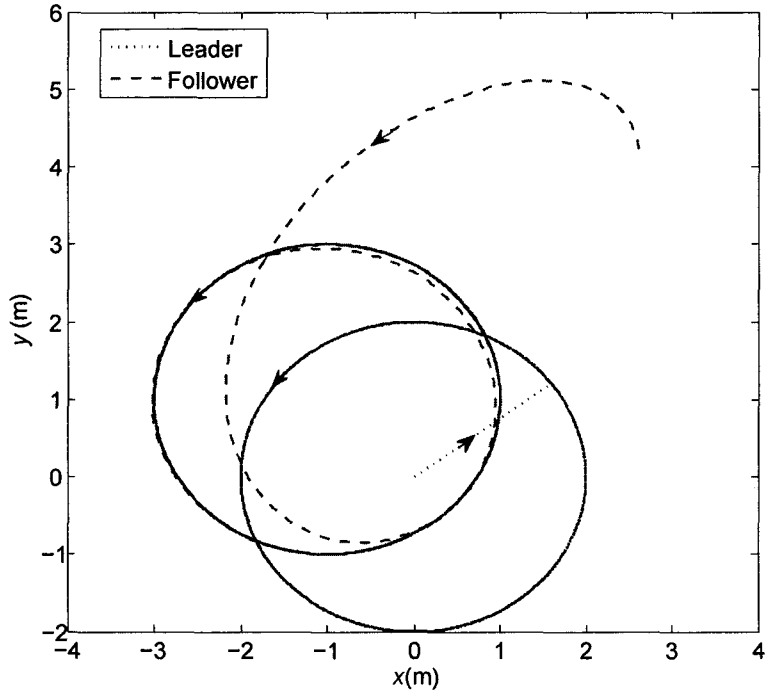

Figure 4.3: The trajectories of the leader and follower in the 2-D plane for the circular trajectory tracking of Example 4.1.

$$P = \begin{bmatrix} 227.3297 & 0 & 71.2285 & 0 \\ 0 & 227.3297 & 0 & 71.2285 \\ 71.2285 & 0 & 78.0058 & 0 \\ 0 & 71.2285 & 0 & 78.0058 \end{bmatrix}$$

$$\lambda_{min}(P) = 49.4791, \quad \delta_1 = 3.4201 \times 10^3, \quad \delta_2 = 9, \quad \varsigma = 3.8730 \times 10^{-4}$$

$$\varsigma_1 = 1.7269 \times 10^3, \quad \sigma = 0.5789, \quad \rho = 0.0013$$

For $T_d = 20$ sec, *the values* ε *and* λ *are chosen to be* 3 *and* 1, *respectively. Thus, using Theorem 4.2:*

$$r = \sqrt{\frac{0.1350}{1 - e^{-0.1\bar{T}}}}$$

For instance, $\bar{T} = 20$ sec, *leads to* $r = 0.3951$; *i.e. the error converges to the ball*

$\mathscr{B}(0.3951)$ *if the tracking trajectory switches every 20* sec. *Figure 4.4 shows the relative position of the follower with respect to the leader in this case, along the x-axis. The desired trajectory* d_x *is also sketched in this figure for comparison. The trajectories in the y direction are shown analogously in Figure 4.5.*

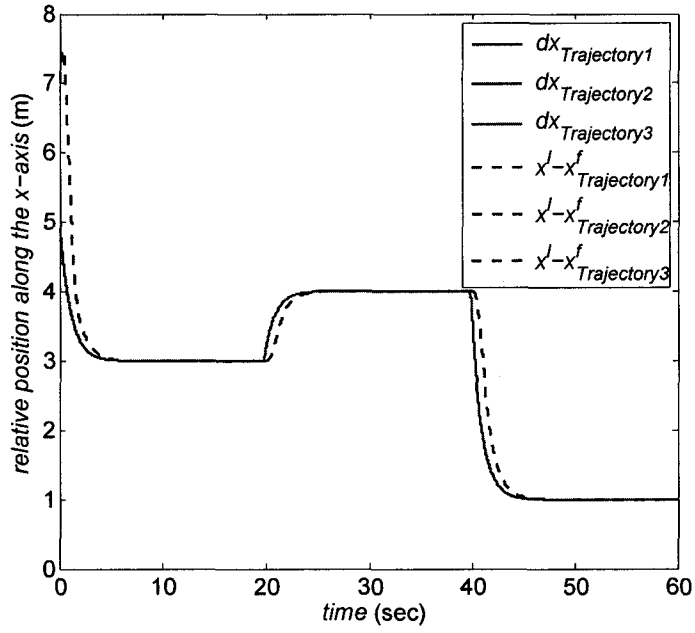

Figure 4.4: The relative position of the follower with respect to the leader along the x-axis for the leader-follower system of Example 4.2 with circular trajectory tracking.

In Figure 4.6, the trajectories of the leader and follower moving toward their desired path are drawn. This figure demonstrates that the agents track their desired path precisely.

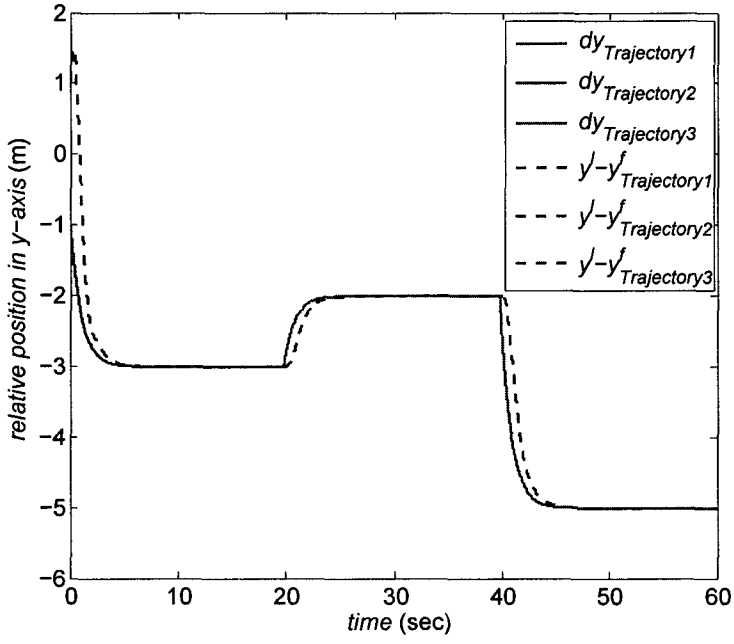

Figure 4.5: The relative position of the follower with respect to the leader along the y-axis for the leader-follower system of Example 4.2 with circular trajectory tracking.

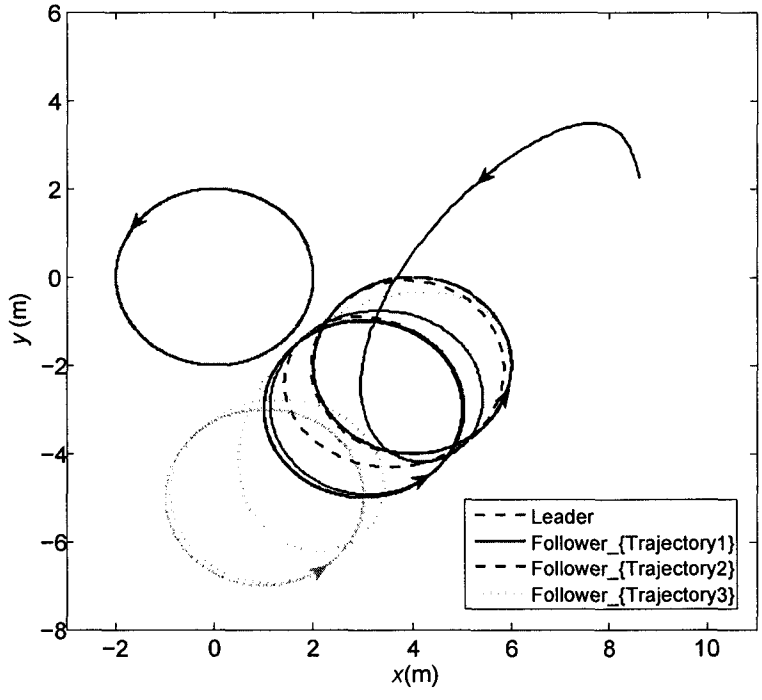

Figure 4.6: The trajectories of the leader and follower in the 2-D plane for the leader-follower of Example 4.2 circular trajectory tracking.

Chapter 5

Conclusions

5.1 Summary

Mobile robots have a wide variety of applications in industry. In this thesis, the trajectory tracking problem using wheeled mobile robots (WMR) is studied. The developed results can be summarized as follows:

In Chapter 2, trajectory tracking by a single WMR is studied. Using linear matrix inequalities (LMI), a proper controller is designed to stabilize the system under different conditions. Input saturation is also addressed by imposing a proper constraint on robot's input. Moreover, upper bounds for the steady-state position and velocity errors are found.

Formation control for a group of mobile unicycle robots is then studied in Chapter 3. Input saturation is also addressed by imposing a proper constraint on the followers' input in the formulation. Stability analysis is provided, and a controller is designed using LMIs to minimize the upper bound of the steady-state errors. Two examples of path following are examined by simulation, which demonstrate the efficacy of the proposed methods.

In Chapter 4, the effect of time delay in formation control with leader-follower structure (studied in Chapter 3) is investigated. Using LMIs, stability criteria for the system with time-varying delay is obtained and upper bounds on the radii of the balls to

which position and velocity errors exponentially converge are given. The result is then extended to the case where the trajectories switch. Using the concepts of *dwell time* and *average dwell time*, upper bounds are obtained for the steady-state position and velocity errors in the formation. Simulations show the effectiveness of the results obtained.

5.2 Future Work

In what follows, some of the possible extensions to the results obtained in this thesis as well as some relevant problems for future study are presented.

- *Obstacle in the environment*: In the present work, an obstacle free environment is considered. However, in real environments there often exist obstacles which need to be considered in designing the controller.

- *Collision avoidance*: Another issue which can be considered as future work is collision avoidance. The controller needs to be equipped with a proper emergency strategy to maintain a sufficiently large distance between any pair of robots.

- *Adaptive Controller*: In Chapter 3, it is assumed that each robot's acceleration bound is known. However, this is not a practical assumption in some applications. One can use an adaptive control scheme to relax this condition. For instance, an adaptive control law of the following form can be used instead of (3.8) for this purpose:

$$u^i = K^i e^i - \frac{B^T P^i e^i}{\|B^T P^i e^i\|}\hat{\Theta}(t) \quad , \quad i \in \{2,...,n\}$$
$$\dot{\hat{\Theta}}(t) = \|e^{iT} P^i B\|$$

  In this case, it is only required to assume that there exists a bound on each robot's acceleration (which could be unknown).

Bibliography

[1] R. Siegwart and I. Nourbakhsh, *Introduction to Autonomous Mobile Robots.* The MIT Press, 2004.

[2] G. Oriolo, A. De Luca, and M. Vendittelli, "WMR control via dynamic feedback linearization: Design, implementation, and experimental validation," *IEEE Transactions on Control Systems Technology*, vol. 10, no. 6, pp. 835–852, 2002.

[3] T. van den Broek, N. van de Wouw, and H. Nijmeijer, "Formation control of unicycle mobile robots: a virtual structure approach," in *Proceedings of Joint* 48^{th} *IEEE Conference on Decision and Control and* 28^{th} *Chinese Control Conference*, pp. 8328–8333, 2009.

[4] L. Consolini, F. Morbidi, D. Prattichizzo, and M. Tosques, "On the control of a leader-follower formation of nonholonomic mobile robots," in *Proceedings of the* 45^{th} *IEEE Conference on Decision and Control*, pp. 5992–5997, 2006.

[5] J. Alexander and J. Maddocks, "On the kinematics of wheeled mobile robots," *The International Journal of Robotics Research*, vol. 8, no. 5, pp. 15–27, 1989.

[6] A. Elkady and T. Sobh, "Design and Implementation of a Multi-sensor Mobile Platform," *Novel Algorithms and Techniques in Telecommunications and Networking*, pp. 367–372, 2010.

[7] A. De Luca and G. Oriolo, "Modelling and control of nonholonomic mechanical systems," *CISM Courses and Lectures on Kinematics and Dynamics of Multi-Body Systems*, vol. 360, pp. 277–342, 1995.

[8] R. Brockett, R. Millman, and H. Sussmann Eds., "Asymptotic stability and feedback stabilization," *Differential Geometric Control Theory,* pp.181-191, 1983.

[9] C. de Wit and O. Sordalen, "Exponential stabilization of mobile robots with nonholonomic constraints," *IEEE Transactions on Automatic Control*, vol. 37, no. 11, pp. 1791–1797, 1992.

[10] M. Aicardi, G. Casalino, A. Bicchi, and A. Balestrino, "Closed loop steering of unicycle like vehicles via lyapunov techniques," *IEEE Robotics Automation Magazine*, vol. 2, no. 1, pp. 27–35, 1995.

[11] O. Sordalen and O. Egeland, "Exponential stabilization of nonholonomic chained systems," *IEEE Transactions on Automatic Control*, vol. 40, no. 1, pp. 35–49, 1995.

[12] R. M'Closkey and R. Murray, "Exponential stabilization of driftless nonlinear control systems using homogeneous feedback," *IEEE Transactions on Automatic Control*, vol. 42, no. 5, pp. 614–628, 1997.

[13] P. Morin and C. Samson, "Application of backstepping techniques to time-varying exponential stabilization of chained systems," *European Journal of Control*, vol. 3, pp. 15–36, 1997.

[14] M. Aicardi, G. Casalino, A. Balestrino, and A. Bicchi, "Closed loop smooth steering of unicycle-like vehicles," in *Proceedings of the* 33^{rd} *IEEE Conference on Decision and Control*, vol. 3, pp. 2455–2458, 1994.

[15] A. Astolfi, "On the stabilization of nonholonomic systems," in *Proceedings of the* 33^{rd} *IEEE Conference on Decision and Control*, vol. 4, pp. 3481–3486, 1994.

[16] A. Astolfi, "Discontinuous control of nonholonomic systems," *Systems and Control Letters*, vol. 27, no. 1, pp. 37–46, 1996.

[17] A. Bloch and S. Drakunov, "Stabilization of a nonholonomic system via sliding modes," in *Proceedings of the* 33^{rd} *IEEE Conference on Decision and Control*, vol. 3, pp. 2961–2963, 1994.

[18] J. Guldner and V. Utkin, "Stabilization of non-holonomic mobile robots using lyapunov functions for navigation and sliding mode control," in *Proceedings of the* 33^{rd} *IEEE Conference on Decision and Control*, vol. 3, pp. 2967–2972, 1994.

[19] C. Samson, "Time-varying feedback stabilization of car-like wheeled mobile robots," *The International Journal of Robotics Research*, vol. 12, no. 1, pp. 55–64, 1993.

[20] C. Samson, "Control of chained systems application to path following and time-varying point-stabilization of mobile robots," *IEEE Transactions on Automatic Control*, vol. 40, no. 1, pp. 64–77, 1995.

[21] C. Samson, "Velocity and torque feedback control of a nonholonomic cart," *Advanced Robot Control*, pp. 125–151, 1991.

[22] J. Coron, "Global asymptotic stabilization for controllable systems without drift," *Mathematics of Control, Signals, and Systems*, vol. 5, no. 3, pp. 295–312, 1992.

[23] C. Samson, "Path following and time-varying feedback stabilization of a wheeled mobile robot," in *International Conference on Control, Automation, Robotics and Vision*, 1992.

[24] R. Closkey, Richard, and M. Murray, "Exponential stabilization of driftless nonlinear control systems via time-varying, homogeneous feedback," *IEEE Trans. on Automatic Control*, vol. 42, pp. 614–628, 1995.

[25] C. Samson and K. Ait-Abderrahim, "Feedback control of a nonholonomic wheeled cart in cartesian space," in *Proceedings of the IEEE International Conference on Robotics and Automation*, vol. 2, pp. 1136–1141, 1991.

[26] A. De Luca and M. Di Benedetto, "Control of nonholonomic systems via dynamic compensation," *Kybernetika*, vol. 29, no. 6, pp. 593–608, 1993.

[27] G. Walsh, D. Tilbury, S. Sastry, R. Murray, and J. Laumond, "Stabilization of trajectories for systems with nonholonomic constraints," *IEEE Transactions on Automatic Control*, vol. 39, no. 1, pp. 216–222, 1994.

[28] C. Rui and N. McClamroch, "Stabilization and asymptotic path tracking of a rolling disk," in *Proceedings of the* 34^{th} *IEEE Conference on Decision and Control*, vol. 4, pp. 4294–4299, 1995.

[29] M. Fliess, J. Lévine, P. Martin, and P. Rouchon, "Design of trajectory stabilizing feedback for driftless at systems," in *Proceedings of the* 3^{rd} *European Control Conference*, pp. 1882–1887, 1995.

[30] B. d'Andrea Novel, G. Campion, and G. Bastin, "Control of nonholonomic wheeled mobile robots by state feedback linearization," *The International Journal of Robotics Research*, vol. 14, no. 6, pp. 543–559, 1995.

[31] Z.-P. Jiang and H. Nijmeijer, "A recursive technique for tracking control of nonholonomic systems in chained form," *IEEE Transactions on Automatic Control*, vol. 44, no. 2, pp. 265–279, 1999.

[32] R. Fierro and F. Lewis, "Control of a nonholonomic mobile robot: backstepping kinematics into dynamics," in *Proceedings of the* 34^{th} *IEEE Conference on Decision and Control*, vol. 4, pp. 3805–3810, 1995.

[33] Z. Jiang and H. Nijmeijer, "Tracking control of mobile robots: a case study in backstepping," *Memorandum-University of Twente Faculty of Applied Mathematics*, 1996.

[34] P. Kokotovic, "The joy of feedback: nonlinear and adaptive," *IEEE Control Systems Magazine*, vol. 12, no. 3, pp. 7–17, 1992.

[35] J. Liu and J. Wu, *Multi-agent Robotic Systems*. CRC Press, 2001.

[36] H. Durrant-Whyte and T. Bailey, "Simultaneous localization and mapping: part I," *IEEE Robotics & Automation Magazine*, vol. 13, no. 2, pp. 99–110, 2006.

[37] Z. Wang, Y. Takano, Y. Hirata, and K. Kosuge, "Decentralized cooperative object transportation by multiple mobile robots with a pushing leader," *Distributed Autonomous Robotic Systems*, pp. 453–462, 2007.

[38] H. Kitano, M. Asada, Y. Kuniyoshi, I. Noda, E. Osawa, and H. Matsubara, "Robocup: A challenge problem for AI and robotics," *Lecture Notes in Computer Science*, pp. 1–19, 1998.

[39] R. Bishop, *Intelligent Vehicle Technology and Trends*. Artech House, 2005.

[40] H. Yamaguchi, "A cooperative hunting behavior by mobile-robot troops," *The International Journal of Robotics Research*, vol. 18, no. 9, pp. 931–940, 1999.

[41] W. Burgard, M. Moors, C. Stachniss, and F. Schneider, "Coordinated multi-robot exploration," *IEEE Transactions on Robotics*, vol. 21, no. 3, pp. 376–386, 2005.

[42] J. Jennings, "Moving furniture with teams of autonomous robots," in *Proceedings of the International Conference on Intelligent Robots and Systems*, vol. 1, pp. 235–242, 1995.

[43] M. Mataric, M. Nilsson, and K. Simsarian, "Cooperative multi-robot box-pushing," in *Proceedings of the 1995 IEEE/RSJ International Conference on Intelligent Robots and Systems*, vol. 3, pp. 556–561, 1995.

[44] D. Stilwell and J. Bay, "Toward the development of a material transport system using swarms of ant-like robots," in *Proceedings of the IEEE International Conference on Robotics and Automation*, vol. 1, pp. 766–771, 1993.

[45] P. Corke, J. Trevelyan, T. Sugar, and V. Kumar, "Control and coordination of multiple mobile robots in manipulation and material handling tasks," *Experimental Robotics VI, Lecture Notes in Control and Information Sciences*, vol. 250, pp. 15–24, 2000.

[46] T. Balch and R. Arkin, "Behavior-based formation control for multirobot teams," *IEEE Transactions on Robotics and Automation*, vol. 14, no. 6, pp. 926–939, 1998.

[47] J. Lawton, R. Beard, B. Young, R. Syst, and A. Tucson, "A decentralized approach to formation maneuvers," *IEEE Transactions on Robotics and Automation*, vol. 19, no. 6, pp. 933–941, 2003.

[48] K. Do and J. Pan, "Nonlinear formation control of unicycle-type mobile robots," *Robotics and Autonomous Systems*, vol. 55, no. 3, pp. 191–204, 2007.

[49] M. Lewis and K. Tan, "High precision formation control of mobile robots using virtual structures," *Autonomous Robots*, vol. 4, no. 4, pp. 387–403, 1997.

[50] J. Desai, J. Ostrowski, and V. Kumar, "Modeling and control of formations of nonholonomic mobile robots," *IEEE Transactions on Robotics and Automation*, vol. 17, no. 6, pp. 905–908, 2001.

[51] X. Li, J. Xiao, and Z. Cai, "Backstepping based multiple mobile robots formation control," in *Proceedings of IEEE/RSJ International Conference on Intelligent Robots and Systems*, pp. 1313–1318, 2005.

[52] J. Sanchez and R. Fierro, "Sliding mode control for robot formations," in *Proceedings of IEEE International Symposium on Intelligent Control*, pp. 438–443, 2003.

[53] T. Barfoot and C. Clark, "Motion planning for formations of mobile robots," *Robotics and Autonomous Systems*, vol. 46, no. 2, pp. 65–78, 2004.

[54] A. Das, R. Fierro, V. Kumar, J. Ostrowski, J. Spletzer, and C. Taylor, "A vision-based formation control framework," *IEEE Transactions on Robotics and Automation*, vol. 18, no. 5, pp. 813–825, 2002.

[55] J. Spletzer, A. Das, R. Fierro, C. Taylor, V. Kumar, and J. Ostrowski, "Cooperative localization and control for multi-robot manipulation," in *Proceedings of IEEE/RSJ International Conference on Intelligent Robots and Systems*, vol. 2, pp. 631–636, 2001.

[56] G. Mariottini, G. Pappas, D. Prattichizzo, and K. Daniilidis, "Vision-based localization of leader-follower formations," in 44^{th} *IEEE Conference on Decision and Control and European Control Conference*, pp. 635–640, 2005.

[57] L. Consolini, F. Morbidi, D. Prattichizzo, and M. Tosques, "A geometric characterization of leader-follower formation control," in *IEEE International Conference on Robotics and Automation*, pp. 2397–2402, 2007.

[58] S. Boyd, L. El Ghaoui, E. Feron, and V. Balakrishnan, *Linear Matrix Inequalities in System and Control Theory*. Society for Industrial Mathematics, 1994.

[59] J. Lygeros, D. Godbole, and S. Sastry, "Verified hybrid controllers for automated vehicles," *IEEE Transactions on Automatic Control*, vol. 43, no. 4, pp. 522–539, 1998.

[60] V. Kharitonov, "Robust stability analysis of time delay systems: A survey," *Annual Reviews in Control*, vol. 23, pp. 185–196, 1999.

[61] S.-I. Niculescu, E. Verriest, L. Dugard, and J.-M. Dion, "Stability and robust stability of time-delay systems: A guided tour," in *Stability and Control of Time-delay Systems* (L. Dugard and E. Verriest, eds.), vol. 228 of *Lecture Notes in Control and Information Sciences*, pp. 1–71, Springer Berlin / Heidelberg, 1998.

[62] S. Mondie and V. Kharitonov, "Exponential estimates for retarded time-delay systems: an LMI approach," in *IEEE Transactions on Automatic Control*, vol. 50, pp. 268–273, 2005.

[63] D. Liberzon and A. Morse, "Basic problems in stability and design of switched systems," *IEEE Control Systems Magazine*, vol. 19, no. 5, pp. 59–70, 1999.

[64] D. Liberzon, *Switching in Systems and Control.* Birkhauser: Boston, 2003.

[65] A. Morse, "Supervisory control of families of linear set-point controllers Part I. Exact matching," *IEEE Transactions on Automatic Control*, vol. 41, no. 10, pp. 1413–1431, 1996.

[66] J. Hespanha and A. Morse, "Stability of switched systems with average dwell-time," in *Proceedings of the* 38^{th} *IEEE Conference on Decision and Control*, vol. 3, pp. 2655–2660, 1999.